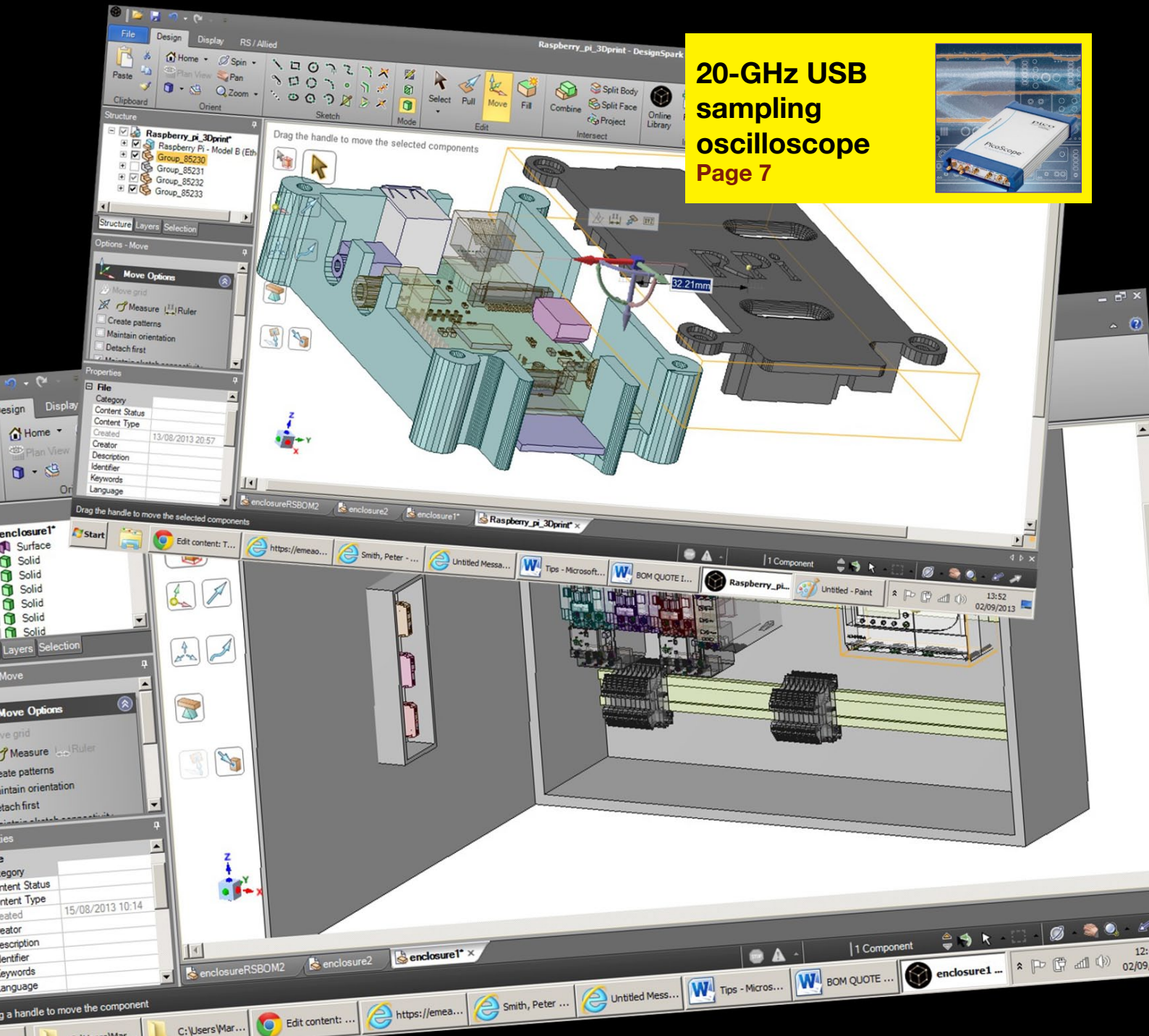


**20-GHz USB
sampling
oscilloscope**
Page 7



Improving noise in wideband fully differential amplifiers
Understanding grounding, shielding, and guarding
Automotive safety and ISO 26262 compiler qualification
10 C language tips for hardware engineers

Page 14
Page 18
Page 26
Page 28

14 Wideband fully differential amplifier noise improved using active match

Since its first appearance in 1999, the single to differential application of wideband fully differential amplifiers (FDAs) has used a resistor to ground as part of the input match at the cost of higher input referred noise voltage. If that resistor could be removed, with an input impedance match set solely by the path into the summing junction, a much lower input referred noise should be possible.

by Michael Steffes, Intersil

18 Understanding grounding, shielding, and guarding in high impedance applications

Inadequate shielding and bad grounding are often blamed when measurements are inaccurate, especially in high impedance applications. In fact, shielding and grounding problems are frequently responsible for measurement errors, but many test system developers aren't quite sure why. Many measurement errors can be traced back to currents from external fields that have become coupled into the measurement test leads

by James Niemann, Keithley Instruments

26 Automotive safety and ISO 26262 qualification of compilers

Microcontroller usage within the automotive industry is widespread with 32-bit devices found in everything from comfort controls, stability and traction control systems through to engine management. Software complexity in automotive electronic control units has also been increasing steadily and has created the need to provide a number of standards frameworks to ensure software code reliability and functional safety.

by Graham Morphey, Wind River

28 10 C language tips for hardware engineers

It can be common for a hardware designer to write code to test that hardware is working. These ten tips for C—still the language of choice—may help the designer avoid basic mistakes that can lead to bugs and maintenance nightmares.

by Jacob Beningo, Beningo Engineering

DEPARTMENTS & COLUMNS

5 EDN.comment

A life of its own

22 Baker's Best

Rally your noise tools for a good offense

23 Teardown 1, and tryout;

WiFi humidity monitor module

by Martin Rowe

37 Teardown 2

Samsung Galaxy Note 3: still the category leader

by TechInsights staff

48 Product Roundup

Industrial 18-bit A/D, Worldwide DVB demodulator, 330 μ F in an MLCC

47 Tales from the Cube

A shock to the circuit

DESIGN IDEAS

32 Per-quadrant linear amplifier distinguishes input polarity

33 Multiple PSUs share load

34 Novel Q-meter

pulse

6 PICs integrate analogue signal chain with 16-bit converters

7 USB 'scope range grows with 20-GHz electrical, 9.5 GHz optical sampling units

7 Free-to-download CAD tool "brings 3D design to every engineer"

8 Directly measuring inductance creates new position/motion sensing opportunities

11 ADI adds mixed-signal control processor for industrial motor and solar inverter designs

11 VDE Certified Library for Infineon MCUs satisfies IEC60730 Class B

12 Online Ada educational resource for the safety-critical software community

12 AMD sets out plans for embedded processor markets

13 Agilent Technologies splits measurement from life-sciences businesses

Cover image

This month's cover depicts screen shots from RS Components' DesignSpark Mechanical 3D CAD package for electronic engineers – see story on page 7

Ever wished for a better bench scope?

The new R&S®RTM: Turn on. Measure.

Easy handling, fast and reliable results – exactly what users expect from a bench oscilloscope. Rohde & Schwarz opens the door to a new world: Work with two screens on one display. Access all functions quickly. Analyze measurement results while others are still booting up. See signals where others just show noise. That's the R&S®RTM.

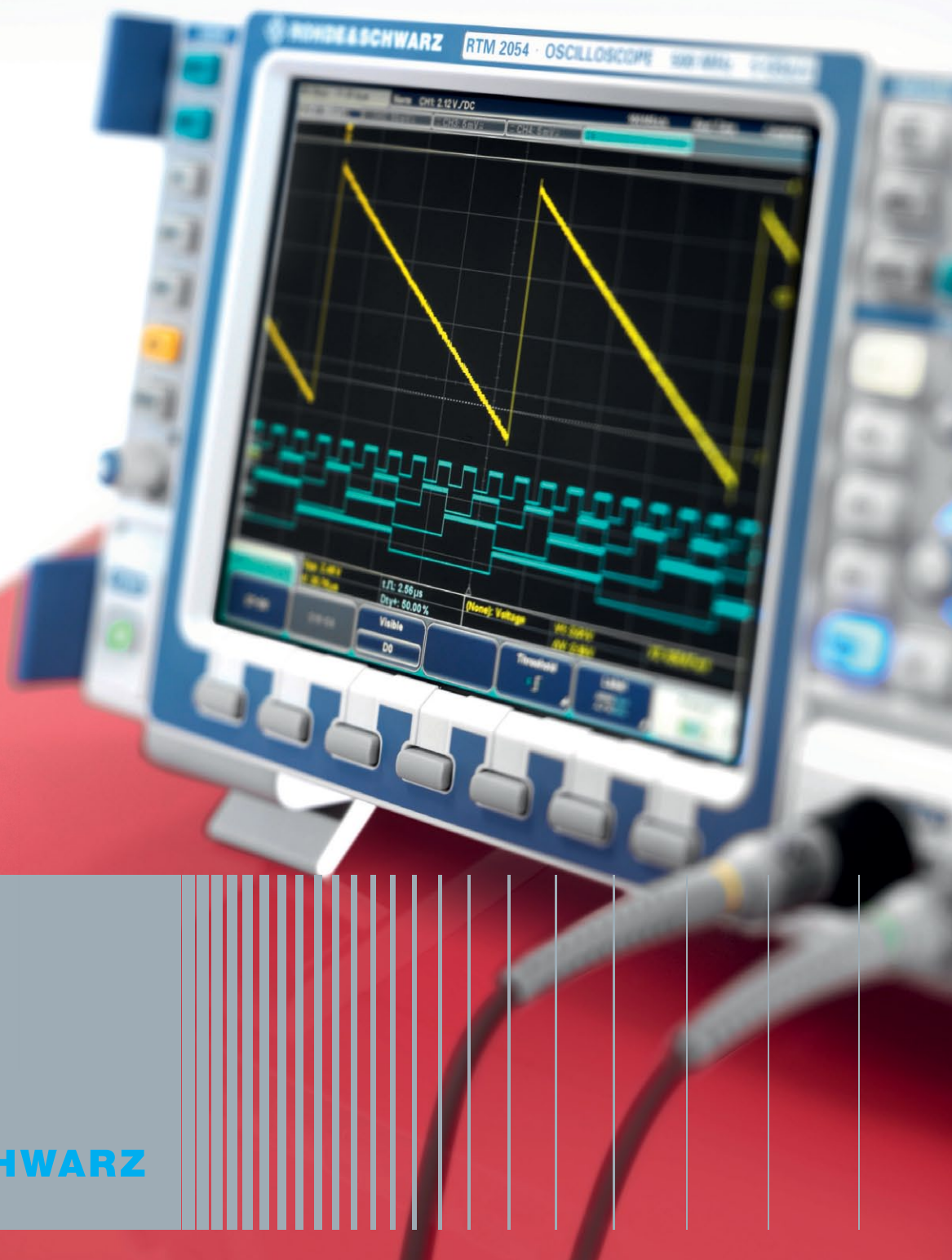
Ever wished there was an easier way? Ever wished for more reliable results? Ever wished you could do your job faster?

Then take a look.

www.scope-of-the-art.com/ad/rtm-video



Please visit us at the
European Microwave Week
in Nuremberg,
hall 7A, booth 106



EDN

europa

OCTOBER 2013
www.edn-europe.com
Issue 10

CONTACTS

PUBLISHER

André Rousselot
+32 27400053
andre.rousselot@eetimes.be

EDITOR-IN-CHIEF

Graham Prophet
+44 7733 457432
edn-editor@eetimes.be

Patrick Mannion

Brand Director EDN Worldwide

CIRCULATION & FINANCE

Luc Desimpel
luc.desimpel@eetimes.be

ADVERTISING PRODUCTION & REPRINTS

Lydia Gijsegom
lydia.gijsegom@eetimes.be

ART MANAGER

Jean-Paul Speliers

ACCOUNTING

Ricardo Pinto Ferreira

EUROPEAN BUSINESS PRESS SA

7 Avenue Reine Astrid
1310 La Hulpe
Tel: +32 (0)2 740 00 50
Fax: +32 (0)2 740 00 59
www.electronics-eetimes.com
VAT Registration: BE 461.357.437
RPM: Nivelles
Company Number: 0461357437

© 2013 E.B.P. SA



EDN-EUROPE is published 11 times in 2013 by European Business Press SA, 7 Avenue Reine Astrid, 1310 La Hulpe, Belgium
Tel: +32-2-740 00 50 Fax: +32-2-740 00 59
email: info@eetimes.be. VAT Registration: BE 461.357.437.
RPM: Nivelles.

It is free to qualified engineers and managers involved in engineering decisions – see:

<http://www.edn-europe.com/subscribe>

Copyright 2013 by European Business Press SA.

All rights reserved. P 304128

SALES CONTACTS

Europe

Daniel Cardon
France, Spain, Portugal
+33 688 27 06 35
cardon.d@gmail.com

Nadia Liefsoens
Belgium
+32-11-224 397
n.liefsoens@fivemedia.be

Nick Walker
UK, Ireland, Israel,
The Netherlands
+44 (0) 1442 864191
nickjwalker@btinternet.com

Victoria & Norbert Hufmann
Germany PLZ 0-3, 60-65, 8-9,
Austria, Eastern Europe
+49 911 93 97 64 42
sales@hufmann.info

Armin Wezel
Germany PLZ 4-5
+49 (0) 30 37445104
armin@eurokom-media.de

Ralf Stegmann
Germany PLZ 66-69, 7
+49 7131 9234-0
r.stegmann@x-media.net

Monika Ailingner
Switzerland
+41-41-850 4424
m.ailingner@marcomedia.ch

Ferruccio Silvera
Italy
+39-02-284 6716
info@silvera.it

Colm Barry & Jeff Draycott
Scandinavia
+46-40-41 41 78
jeff.draycott@womp-int.com
colm.barry@telia.com

USA & Canada

Todd A. Bria
West
+1 831 477 2075
tbria@globalmediasales.com

Jim Lees
PA, NJ & NY
+1-610-626 0540
jim@leesmedia.com

Steve Priessman
East, Midwest,
South Central
& Canada
+1-630-420 8744
steve@stevenpriessman.com

Lesley Harmoning
East, Midwest,
South Central
& Canada
+1-218.686.6438
lesleyharmoning@gmail.com

Asia

Masaya Ishida
Japan
+81-3-6824-9386
Mlshida@mx.itmedia.co.jp

Grace Wu
Asian Sources Publications
Asia
(886-2) 2712-6877
wug@globalsources.com

John Ng
Asian Sources Publications
Asia
(86-755) 8828 – 2656
jng@globalsources.com

A LIFE OF ITS OWN

At the beginning of this month (October), the semiconductor industry analyst company Future Horizons held the 2013 incarnation of its International Electronics Forum: a combination of wide-ranging futurology conference and networking opportunity for the very-best-connected of semiconductor industry executives. This year's theme was, "Entering The Sub-20nm Era ... 'Business As Usual' OR 'It's Different This Time?'" Future Horizons' founder Malcolm Penn paints a picture of an industry, as he puts it, "brazenly" about to enter the era of sub-20-nm silicon manufacture, at the same time as the entire chip sector faces the combination of a global economic recession, together with "mega-shifts" in its own domain; the move away from a PC-dominated business to one dependent on smart portable devices being the main, but far from the only, example.

Topics ranged from new materials (the currently ultra-cool graphene, for example), challenges in design methodologies, new applications domains, and possible changes to the business model. Subjects as diverse as doing business in Russia and Africa, to modelling the human brain were addressed, in addition to the stock-in-trade subjects of the semiconductor world: how to carry the momentum of the industry onwards through the 20-nm 'barrier'. There were hints of "are we approaching the end of the reign of Moore's Law?" - but semiconductor pundits have learned to be very careful of forecasting that eventuality, as silicon technology has swept right on through several predicted end-points. The Moore's Law party, in terms of shrinking "conventional" structures, has to come to an end some time soon, of course; the quantum-mechanical properties of diminishing numbers of atoms in a drawn element will see to that.

But there's not much reason to suppose that will bring us to any sort of crisis. Moore's Law has largely been an economic one; at any time in the last half-century (or so) it has asked, "what's the cheapest way to buy another step in computing power?" - and for all those years the answer has been, "shrink the silicon process." If that's no longer the answer, then some other material, or technique, or completely orthogonal approach, will step forward to take up the race. If that seems a little glib, it's expressed in a more thoroughly-argued way by US inventor and entrepreneur (many times over, on both counts) Ray Kurzweil. He holds that the unit cost of computing resource has been declining on a logarithmic path (or, that the same power has been increasing exponentially, which amounts to the same thing) since long before there was a semiconductor industry, and will do so long after we stop trying to get integer numbers of silicon atoms to do our bidding.

In this view, Moore's Law has merely been the handmaiden of that broader-scale process for 50 or 60 years, and we can no more ask it to pause while we wait for the global economic situation to settle down a bit, than we might stand on the shore and hold back the tides. If we take this literally, then from the point of view of those applying the computing resource, we can stop worrying about whether 20 nm, 16 nm or any other number of nanometres represents some sort of end-point, and assume that as time goes by, ever-more powerful devices will continue to become available to us. Cavalier as that sounds, it is an attitude that would have served us well over those same decades. The technology and the business model is a dynamic one; it is not a stepwise process in which you can decide that any given plateau is good enough, and you don't have to follow the trend line any more.

Kurzweil and those of similar outlook see the same process at work in many different areas of technology - although the clock rate, the time between ticks that mark the doubling of performance, can surely vary greatly. Centuries before, the economist Adam Smith wrote of the "invisible hand" that guides economic processes - he meant something rather different, but it does appear that once a given technology is set in motion, it acquires a momentum of its own that drives its progress. Perhaps we should stop worrying about the economic situation and simply concentrate on ways to use all of the wave of ever-cheaper computing power that's coming our way.



- searches all
electronics sites

- displays only
electronics
results

- is available on
your mobile



pulse

PICs integrate analogue signal chain with 16-bit converters

Microcontroller is its first to integrate a 16-bit ADC, 10 Msps ADC, DAC, USB and LCD on a single device. The PIC24FJ128GC010 provides intelligent analogue and Microchip's eXtreme Low Power (XLP) for portable medical and industrial applications; it includes Microchip's first on-chip precision 16-bit ADC.

This PIC family is an analogue system on a chip that integrates a full analogue signal chain, including precision 16-bit ADC and 10 Msps 12-bit ADC, plus a 10-bit DAC and dual operational amplifiers, comparators and voltage references, along with eXtreme Low Power (XLP) technology for extended battery life in portable medical and industrial applications. The device represents a much greater degree of analogue functionality than has previously been integrated with a PIC core, Microchip says, and the first 16-bit sigma-delta precision ADC available in such a chip. In fact, the ADC

is based on a 22-bit architecture, with performance scaled back for noise reasons. All of the analogue design has been done in-house at Microchip and the close integration means that key analogue parameters are all settable in software (register-based) and can be changed on-the-fly if necessary. You would normally configure the analogue circuitry as part of system startup routines. All issues that would normally challenge the designer – of analogue issues such as layout and its effect on noise and signal integrity – are resolved for the user, at chip level, Microchip

says. A full interconnect matrix is provided to route internal connections and to map pins to the outside world. This combination of analogue integration and low power consumption, the company says, reduces system cost and noise, and improves signal throughput in applications which include portable medical monitoring devices such as

mTouch peripheral. Function blocks on the MCU include an 8-channel DMA controller to move data to the converters without CPU intervention. Microchip asserts that the integration of a 16-bit ADC, USB and LCD into a single low-power MCU allows for very small form-factor battery-powered applica-

tions, and represents a significant cost reduction over a multi-chip implementation. The saved board area is greater than just the separate components that you don't need: you can also dispense with shielding and guarding around sensitive analogue tracks, that all requires area. The PIC24FJ128GC010 family is supported by Microchip's Starter Kit for PIC24F, DM240015 which is being offered for a special introductory price of \$89.99 for a limited time. This kit is focused on the family's integrated analogue to preserve signal integrity. It provides 95% of what designers need to develop a handheld analogue prototype - all you

need to do is add sensors. Among the supporting tools is a battery life estimator that takes a realistic view of analogue circuitry and processor cycles to predict life for a portable product concept. PIC24FJ128GC010 (128 kB Flash) and PIC24FJ64GC010 (64 kB Flash) are available in 100-pin TQFP and 121-pin BGA packages. PIC24FJ128GC006 (128 kB Flash) and PIC24FJ64GC006 (64 kB Flash) are available in 64-pin TQFP and QFN packages.

Microchip
www.microchip.com/get/6T4J



Microchip cites a blood glucose meter as a typical application of the "analogue system PIC"

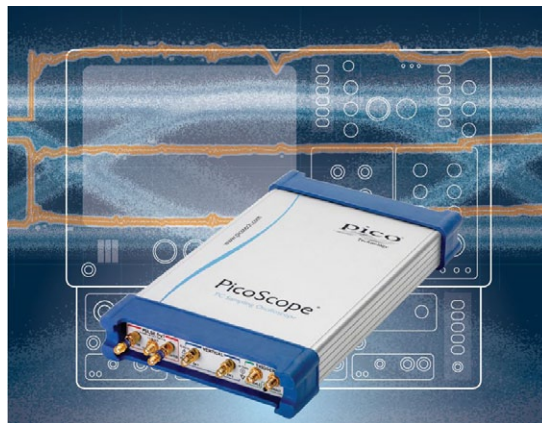
blood glucose meters and blood pressure monitors; as well as industrial applications and portable monitoring devices, such as voltage and current monitors, gas sensors and high-speed sensor arrays. The chip family includes an integrated LCD display driver that provides the ability to drive up to 472 segments with displays that include scrolling alphanumeric banners. Integrated USB supports the uploading of clinical data for medical equipment and can act as a service/data port for industrial equipment. Capacitive touch sensing is supported with an on-chip

USB 'scope range grows with 20-GHz electrical, 9.5 GHz optical sampling units

Pico Technology, designers of USB modular scopes that use PCs or laptops for display and control functions, has expanded its range with the PicoScope 9300 Series TDR/TDT sampling oscilloscopes, for use with repetitive signals. The 9300s can perform time-domain reflectometry and transmission mismatch and network analysis on high-frequency cables, PCBs, backplanes and interconnections. Their built-in differential fast edge generators have a rise time of 65 psec at up to 6V (PicoScope 9311) or 40 psec at over 250 mV (PicoScope 9312, via plug-in pulse heads), providing a typical distance-to-fault resolution down to 10 mm.

“The PicoScope 9300 Series are the only compact, full-featured PC-based sampling oscilloscopes on the market,” claims Alan Tong, Managing Director, Pico Technology. “Their specifications and features are a match for traditional full-sized bench top instruments but at a fraction of the cost.” The TDR/TDT models are full-featured sampling oscilloscopes, so can be used for pre-compliance tests, fault-finding and margin testing on serial data signals such as 10 Gb Ethernet, SONET/SDH STM64 and FEC1071, 10x Fibre Channel, InfiniBand and PCI Express. The scopes also have LAN and USB interfaces, and advanced large-screen display features such as colour and density profiling, multiple trace windows, histograms, multiple measurements and statistics. With a sampling rate of 1 Msample/sec, they can build waveforms and persistence displays faster than other sampling oscilloscopes.

The small footprint of the PicoScope 9300 scopes allows them to be positioned close to the device or port under test, on the bench or in the field, without pull-out sampling modules or



These 20-GHz sampling 'scopes for repetitive waveforms u sts and USB connections.

lossy extension cables. Specification highlights include: 17.5 psec input rise time, dual 16-bit, 60 dB dynamic range ADCs, 5 psec/div dual timebase, 14 GHz trigger bandwidth, built-in clock recovery up to 11.3 Gb/sec, and time interval resolution of 64 fsec. Typical input noise is 1.5 mV RMS at full bandwidth, with trigger jitter of 1.8 psec RMS and recovered clock jitter of 1 psec RMS.

The company's PicoSample software has been updated for the new oscilloscopes, extending the range of controls with intuitive graphics, click-and-drag operations and measurement labels to simplify and speed up operation. The flexible layout displays only the controls and menus you need, leaving the maximum possible space for your data. A suite of measurement and analysis functions contains 61 math operations, 138 automatic measurements and 167 standard comms masks from 1.54 Mb/sec to 12.5 Gb/sec. PicoSample 3 is compatible with all 32-bit and 64-bit versions of Microsoft Windows from Windows XP to Windows 8.

The PicoScope 9300 Series cost €13,930/£11,512 for the PicoScope 9311 and €16,423 / £13,573 for the PicoScope 9312, including all hardware, accessories and software. A demonstration copy of the software can be downloaded from the company's website.

In the same release is an optical sampling derivative 'scope, the 9321, that integrates a 9.5 GHz optical fibre-to-electrical converter with the two-channel, 20 GHz PC sampling 'scope. This extends Pico Technology's serial data and eye diagram visualisation to fibre optic data systems with bit rates up to 11 Gb/sec and includes clock recovery. The PicoScope 9300 platform is the same 20 GHz electrical bandwidth sampling unit, so all of the same tests can be carried out with the 9321 as the 9311/12. The 9321 optical unit costs €21,630/£17,876; a range of standard SMA pulse shaping filters is also available.

Pico Technology
www.picotech.com

Free-to-download CAD tool “brings 3D design to every engineer”

RS Components has introduced DesignSpark Mechanical, a software package that makes 3D mechanical design, available to engineers beyond the established specialist who currently work in 3D; the package is, says RS, free, fast and intuitive, opening new possibilities from concept design through to manufacturing.

DesignSpark Mechanical is a 3D solid modelling and assembly tool, developed in conjunction with SpaceClaim, provider of “flexible and affordable” 3D modelling software. RS is present-

ing the package as a significant step in the evolution of its DesignSpark online resource hub, and is making it available worldwide in 12 languages.

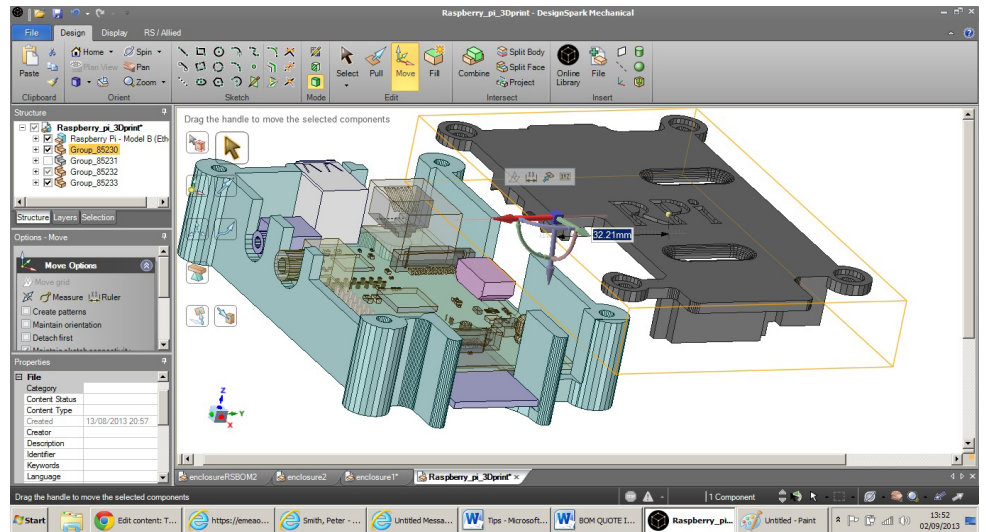
The availability of DesignSpark Mechanical overcomes, RS adds, two major barriers to entry faced by potential users who do not currently have access to a 3D design solution, but who could benefit from the use of 3D modelling to quickly develop sophisticated concepts and products. These impediments are the prohibitive costs and the considerable investment in learning time associated with traditional 3D CAD tools. DesignSpark Mechanical is free, and its authors say its simplicity of use means that engineers and others involved in product development can become fully conversant with the software within minutes, rather than the weeks or months required to become skilled with traditional 3D CAD tools.

The software employs the same use paradigm as SpaceClaim's own product – you manipulate geometry with four basic actions that have more in common with established Windows and mobile-device operation than with traditional CAD. RS believes that using DesignSpark Mechanical early in the design cycle can eliminate much of the time-consuming rework associated with traditional product development processes. The package can exchange data with component databases and with DesignSpark PCB (or in .IDF from many other tools), and can export files in .STL format to generate prototypes on 3D printers.

With access to more than 38,000 3D models in the DesignSpark online component library, DesignSpark Mechanical gives all engineers the ability to undertake an end-to-end design with professional-grade modelling tools that are at zero cost. RS has also collaborated with 3D content company TraceParts to provide access to millions of models from the online tracepartsonline.net CAD portal in DesignSpark Mechanical format.

“RS is partnering with SpaceClaim to launch DesignSpark Mechanical, which combines the power and ease-of-use of direct modelling technology from SpaceClaim with access to the massive RS library of standard parts,” said Rich Moore, vice president of business development for SpaceClaim. “Feature-based CAD is more difficult to learn and with DesignSpark Mechanical, users can rapidly create 3D models to accelerate engineering design and improve their competitive advantage.” He adds that SpaceClaim is both a product, and a platform, and the the software developed for RS constitutes a focussed set of capabilities aimed at the broad range of electronic design, industrial and mechanical design engineers in RS' customer base.

DesignSpark Mechanical employs a methodology called ‘direct modelling’, which is very different from traditional feature- or parametric-based 3D CAD software. The tool uses simple ges-



SpaceClaim, who wrote DesignSpark Mechanical for RS, says that it uses a design approach much more in tune with the electronic systems designer than is the case for conventional CAD.

tures that enable real-time editing and instant feedback, making it possible for engineers and others to create geometry and easily explore ideas and product concepts in 3D. All basic designs can be achieved quickly and easily via the use of the software's four basic tools – Pull, Move, Fill and Combine – in addition to its employment of familiar Windows keyboard shortcuts such as cut/paste, undo/redo, which makes it highly intuitive for new users.

The software can also be used as a complementary 3D tool in the product development process for the creation of early concept designs, for instance, alongside 3D CAD tools that are already in use today. The tool can remove bottlenecks in the early design process by allowing changes and additions in seconds, rather than having to wait for the CAD department using the traditional 3D tools to rework the design.

DesignSpark Mechanical is available for free download via www.designspark.com/mechanical, with support available through the DesignSpark community at www.designspark.com

Directly measuring inductance creates new position/motion sensing opportunities

Texas Instruments claims to have created an entirely new class of data converter, with its Inductance-to-digital converter, which the company believes will fundamentally change position and motion sensing, based on a coil stimulating a target, or detecting deformation of an inductor. The inductance-to-digital converter (“LDC”) offers, in fact, two modes of detection, and that is detection of anything that possesses inductance: which can mean, anything that is conductive. In one mode, a sensor coil excites eddy-currents in a conductive target, which can be as simple as a piece of wire or a metal plate. Using a frequency range of 5 kHz to 5 MHz, the chip sets up resonance in the tank circuit of which the (electrically-unconnected) target forms a part. Any changes in

the position or orientation or orientation of the target will alter the eddy-current losses; that change can be detected by the LDC to 16-bit resolution. In the second mode, the chip directly measures changes the inductance of a conductive element to which it is connected, by measuring frequency shifts; in this mode it achieves 24-bit resolution. Reference to inductance leads naturally to imagining the connected element as a coil; any distortion in the helix is detectable; so a spring can be its own load sensor. 24-bit sensitivity means that, to quote one example cited by TI, changes in the inductance of a bedspring can detect the breathing of the occupant of the bed. This lies behind TI's claim that the LDC can use coils and springs as inductive sensors to deliver higher resolution,

While the world benefits from what's new,
IEEE can focus you on what's next.

Develop for tomorrow with
today's most-cited research.



Over 3 million full-text technical documents
can power your R&D and speed time to market.

- IEEE Journals and Conference Proceedings
- IEEE Standards
- IEEE-Wiley eBooks Library
- IEEE eLearning Library
- Plus content from select publishing partners

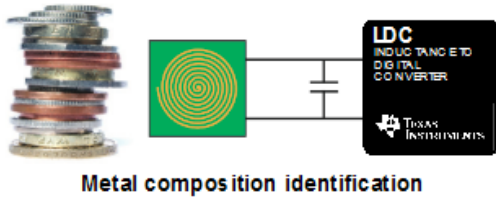
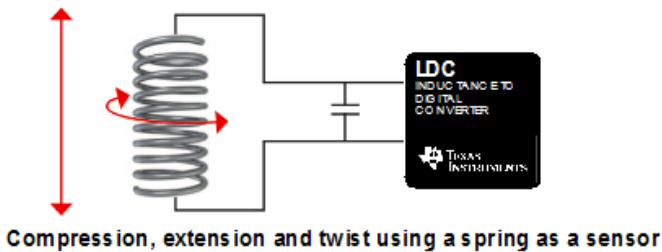
IEEE Xplore® Digital Library

Discover a smarter research experience.

Request a Free Trial
www.ieee.org/tryieeexplore

Follow IEEE Xplore on  

 **IEEE**
Advancing Technology
for Humanity



This illustration shows the two basic modes of using the inductance-to-digital converter

increased reliability, and greater flexibility than existing sensing solutions at a lower system cost. More generally, inductive sensing is a contactless sensing technology that can be used to measure the position, motion, or composition of a metal or conductive target, as well as detect the compression, extension or twist of a spring.

TI says that in many ways inductive sensing is complementary to capacitive sensing; capacitive sensing reacts “to everything” (with high sensitivity) whereas inductive sensing offers high selectivity – at short range. In the industrial arena, inductive sensing is well-known, but has generally required you to implement your own means of measuring inductance and inferring the quantity you want to measure. Lack of an integrated solution has limited applications in consumer and automotive products, TI adds.

Applications for inductive sensing, TI says, range from simple push buttons, knobs, and on/off switches to high-resolution heart rate monitors, turbine flow meters, and high-speed motor/gear controllers. Given their versatility, LDCs can be used in many different markets, including automotive, white goods, consumer electronics, mobile devices, computing, industrial, and medical.

LDC technology enables you to create sensors using low-cost and readily available PCB traces or metal springs. LDCs provide high-resolution sensing of any metal or conductor – including the human body.

You can achieve sub-micron resolution in position-sensing applications with 16-bit resonance impedance and 24-bit inductance values. Increased reliability comes from contactless sensing that is immune to nonconductive contaminants, such as oil, dirt and dust, which can shorten equipment life and interfere with optical detection. Flexibility comes with being able to locate the sensor remotely from the electronics, where PCBs cannot be placed. Use of low-cost sensors and targets, without magnets, cuts system costs. The LDC supports pressed foil or conductive ink targets, offering endless opportunities for creative and innovative system design. It consumes less than 8.5 mW during standard operation and less than 1.25 mW in standby mode. You can achieve lower cost and power than either a Hall-effect or optical system, TI claims.

Very high precision is available over short distances; short means, within one-half to one diameter of the sensing coil. The

effect is always available in a similar ratio; so, a TI spokesman says, you can get 0.1-mm accuracy at 1 mm distance from a 1-cm-diameter coil; or 1-mm accuracy, 1 cm away from a 10-cm coil. In effect, the chip replaces the magnet in a traditional configuration, acting as a high-frequency electromagnet, and seeking disturbances in the field.

The illustration shows the output of a system in which a steel plate is claimed in proximity to a PCB-coil – a resolution of around 5 µm is achieved at 8 mm distance. The graph is a statistical spread of the measurements, which may have some electrical noise component, and/or represent some minute mechanical perturbations of the system. Regard it, TI says, as the system-level noise floor of the setup. One of the characteristics of the technique is that as the distance to the target decreases, the available dynamic range also gets lower. You can measure the amount of metal that is over a coil, so a shaped metal target can directly yield lateral displacement – or velocity/acceleration. Where a Hall-effect detector might need a ferrous gear-tooth sensing wheel, with rectangular teeth, the LDC can resolve a non-metallic target with shaped teeth, and infer fractional-tooth position by interpreting the shaping.

Output data rate depends on the sensor frequency, and a settable parameter “response time” (which configures a digital filter). For example, according to the data sheet; if the sensor frequency is the maximum of 5 MHz and the response time is set at the minimum value, the data rate is maximised at 78.125 ksamples/sec.

To assist with design of the inductive sensors, TI has added a dedicated section to its Webench on-line tools, that calculates dimensions and simulates circuit behaviour for a variety of sensor configurations.

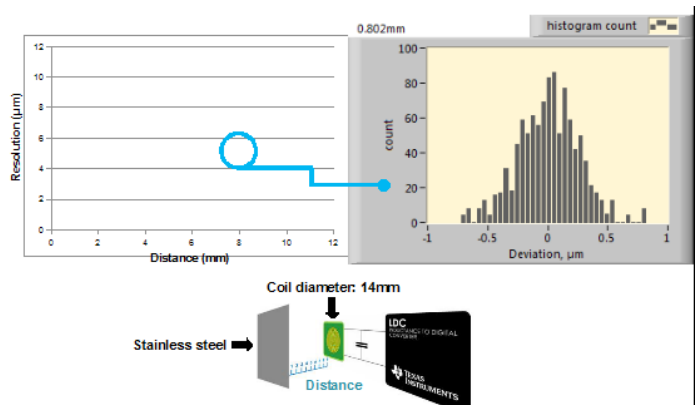
The LDC1000EVM evaluation module, which includes an MSP430F5528 microcontroller (MCU), is available for \$29.00: an Inductive Sensing Forum has been set up in the TI E2E Community, where engineers can ask questions and get answers from TI experts.

The LDC1000, in a 16-pin, 4 by 5-mm SON package costs \$2.95 (1,000) An automotive-qualified version will be available the first half of 2014.

TI

www.ti.com / www.ti.com/lcd1000-pr-eu

There is a video demonstration of the LDC1000 here; and you can download the “**Guide to Inductive Sensing**” infographic to learn how to build a sensor using an LDC.



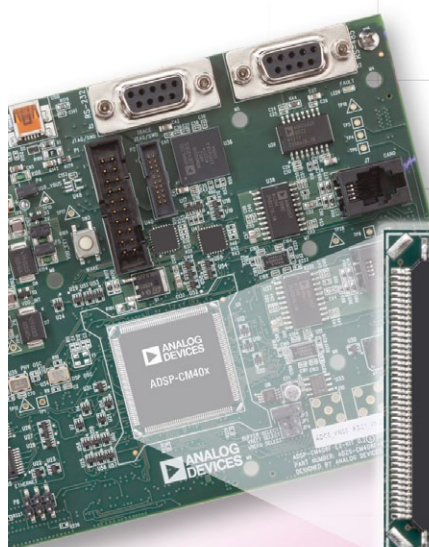
Illustrating the sensitivity of the inductance measurement technique to minute movements.

ADI adds mixed-signal control processor for industrial motor and solar inverter designs

Analog Devices' ADSP-CM40x integrates a high-precision A/D converter and a fast ARM Cortex-M4 to meet the performance demands of next-generation industrial control and electrical grid equipment.

The mixed-signal control processor integrates an embedded dual 16-bit A/D converter with up to 14 bits of accuracy together with a 240-MHz floating-point ARM Cortex-M4 processor core. Analog anticipates applications for highly accurate, closed-loop control in servo, motor-drive, solar photo-voltaic (PV) inverter and other embedded industrial functions. The company says that the M4 core provides the performance needed for this sector, but that a typical design will leave ample headroom in the core to run the application as well as the power conversion algorithms.

The ADSP-CM40x series is the first of a new generation of mixed-signal control processors being developed by Analog Devices for precision control applications. In addition to its analogue conversion performance and 380-nsec conversion speeds, the ADSP-CM40x provides a number of other features such as a full sinc filter implementation to interface directly to isolated sigma-delta modulators (AD7400A/AD7401A) which are used in shunt-based current sensing system architectures. The availability of an on-chip sinc filter eliminates the cost and engineering resources required to implement that function in an FPGA. While the architecture assumes an external sigma-delta converter will be used for high-precision current sensing, other blocks that match the chip to the industrial environment are



- 240 MHz ARM® Cortex™-M4 Core
- Dual 16-bit ADC w/14-bit Accuracy
- 380 ns Conversion Speeds
- Integrated Sinc Filters

included, such as communications via real-time Ethernet and USB.

ADI has provided integration with the MathWorks tool set. Through the use of MathWorks' ARM Cortex-M optimised Embedded Coder and tool suites, you can take designs from simulation to productised code implementation in an embedded platform. "Through optimised code generation, device drivers and compiler suites, [the] ADSP-CM40x series enable engineers to plug their designs directly into an environment for model-based design using MATLAB and Simulink software, streamlining the workflow from system modelling to controller deployment

to verification and certification," said Tom Erkkinen, products manager, MathWorks. "This structure defines a complete model-based development platform, allowing engineers to focus on faster development of more efficient systems." While the chip can support a degree of safety-oriented design, this version is not dual-core and has no lock-step operation facility, something that ADI hints might be under consideration.

The solar inverter sector is mentioned as a particular target market,

where the trade-off of a sigma-delta converter's speed – not vital in solar PV – for accuracy will be useful in measuring small increments in a very large range, such as in a high-voltage panel array. The output PWM is flexible in timing, ADI says, but the the company has not chosen to implement detailed tuning of IGBT drive waveforms in this device, and that that might yield another increment in efficiency at a later stage.

ADSP-CM40x costs from \$8.14 (1000 per year).

Analog Devices
www.analog.com

VDE Certified Library for Infineon MCUs satisfies IEC60730 Class B

Infineon has a free VDE certified IEC 60730 self-test library for its XMC1000 and XMC4000 families of industrial 32-bit microcontrollers that offers a fast route to safety-compliant appliances.

With the Infineon Class B library packages, the XMC1000 and XMC4000 families satisfy the requirements defined by IEC 60730 Class B, a standard which has been mandatory since

October 2007 for the safety of household appliances sold in Europe. The standard affects all electronic controls used in home appliances to prevent unsafe operation, e.g. cookers and motor controls for dishwashers, refrigerators, dryers, cloth washers, and fans. In order to get household products certified, embedded microcontrollers have to perform certain self-tests to prove that they are running correctly at all times.

VDE is the German Association for Electrical, Electronic & Information Technologies and one of Europe's largest technical and scientific associations with more than 36,000 members. VDE provides an independent test and certification institute.

XMC microcontrollers integrate all hardware functions to meet Class B requirements, such as a CRC engine and watchdog

with an independent clock. Combining these with the free self-test software library that offers detailed tests and diagnostic methods, XMC microcontrollers support an effective approach to implement the related safety functionality for Class B certification. In addition to the startup tests such as reset mechanism, memory test (RAM, Flash, ECC and parity), clock system test (source, PLL and oscillators) and core tests, a set of runtime tests is provided. As a consequence, test routines on the CPU and on the microcontroller peripherals evaluated by a safety period monitoring mechanism ensure exact implementation of the Class B requirements with extremely high diagnostic coverage. The modular library design allows easy integration of startup tests and runtime tests into the application software or the customers' software designs.

Developed to replace low-end 8-bit industrial MCUs, XMC1000 microcontrollers offer 32-bit performance at 8-bit prices and are targeted for use in household appliances. XMC1000 microcontrollers combine the ARM Cortex-M0 processor with an advanced 32-bit peripheral set. Target applications include sensor and actuator systems, LED lighting, digital power conversion, such as uninterruptible power supplies, and simple motor drives, such as those used in household appliances, pumps, fans and e-bikes.

XMC4000 microcontrollers are based on the ARM Cortex-M4 processor and offer application-optimised peripherals and real-time capability for electric drives, solar inverters and the automation of manufacturing and buildings. With flexible timers, fast ADCs, fast and robust Flash memory, extended temperature ranges of up to 125C and support for a large number of communications protocols they are well-suited for applications that improve energy efficiency.

Both the XMC1000 and XMC4000 are supported by the free, integrated development platform DAVE, which makes development of application-oriented software user-friendly and eases transition between the XMC1000 and XMC4000 families.

Embedded systems solutions provider Hitex provides the Class B software library for the XMC microcontrollers and supports XMC users to receive certification through VDE.

The free software library supporting single-channel architecture with periodic self-test routines to be called at system startup or periodically at system run time is available at

www.infineon.com/classB

XMC4000 and XMC1000 families; www.infineon.com/xmc
DAVE is available as a free download; www.infineon.com/dave

Hitex
www.hitex.com

Online Ada educational resource for the safety-critical software community

AdaCore's AdaCore University is a free, web-based resource centre for anyone interested in learning about, or how to program in, the standards-based Ada programming language. The website offers pre-recorded courses and other learning materials on Ada, with access to AdaCore's open

source GNAT Ada toolset for writing and running example programs. It also utilises the latest in website design and learning tool features. Students at all levels of experience and expertise can begin writing programs quickly and can proceed at their own pace.

AdaCore University courses educate through examples, allowing students to see, understand and experiment with most features of the Ada programming language. Drawing on the experience and teaching credentials of Ada experts such as New York University Emeritus Professors and AdaCore founders Robert Dewar and Edmond Schonberg, the courses explain Ada's technical concepts with insight into the rationale and usage of particular features.

The initial curriculum includes two courses:

- Ada 001, "Overview" – a module that presents an overall picture of the language and that allows students to write small programs; and
- Ada 002, "Basic Concepts" – the first in a formal series of Ada classes, introducing basic Ada programming concepts and allowing students to write programs based on these features. Both of these modules, and all future courses, provide sources and installation instructions for all learning materials and tools. The courses cover the latest version of the Ada language (Ada 2012), and students have access to AdaCore's GNAT Ada development environment and programming tools. The AdaCore University website also hosts a number of technical papers on Ada, offering insight into particular aspects of the language's design and usage.

AdaCore University is an ongoing, live project that will be expanded to include more advanced courses on Ada, and SPARK 2014 – an Ada-based programming language designed for high-integrity software (i.e., where reliability is essential and where safety and/or security certification may be required). AdaCore University is endorsed by leading non-profit organisations dedicated to sustaining and promoting the Ada programming language, including the Ada Resource Association, SIGAda, Ada Deutschland, Ada France and Ada-Europe.

AdaCore University
<http://u.adacore.com>

AMD sets out plans for embedded processor markets

AMD is to offer embedded system designers a range that will include ARM or x86 SoC, in APU or CPU options coupled with AMD Radeon graphics. AMD's range includes two x86 accelerated processing units (APUs) and central processing units (CPUs), a first look at a high-performance ARM system-on-chip (SoC) and a new family of discrete AMD Embedded Radeon graphics processing units (GPUs) expected to launch in 2014. These additions provide the embedded industry's engineering community with more choices to match their exact design needs, and are designed to offer improvements in performance-per-watt and performance-per-dollar. Together with the recent launch of the AMD Embedded G-Series SoC family with its high performance-per-watt low-power multicore APUs, these latest additions to the embedded product roadmap further signify, the company says, a strategic push by AMD to

focus on the high-growth embedded market. In 2014, AMD plans to bring to market two new high-performance AMD Embedded R-Series processor families: the "Hierofalcon" CPU SoC family based on the ARM Cortex-A57 architecture and the "Bald Eagle" APU and CPU offering based on the x86 microprocessor architecture codenamed "Steamroller." The upcoming "Steppe Eagle" APU SoC is designed to provide improved performance while extending the low-power characteristics of the current AMD Embedded G-Series SoC family. In addition, "Adelaar" will bring to market the first discrete GPU based on AMD Graphics Core Next architecture for embedded systems.

"Hierofalcon" is the first 64-bit ARM-based platform from AMD targeting embedded data centre applications, communications infrastructure and industrial solutions. It will include up to eight ARM Cortex-A57 CPUs expected to run up to 2.0 GHz, and provides high-performance memory with two 64-bit DDR3/4 channels with error correction code (ECC) for high reliability applications. The highly integrated SoC includes 10 Gb KR Ethernet and PCI-Express Gen 3 for high-speed network connectivity, making it ideal for control plane applications. The "Hierofalcon" series also provides enhanced security with support for ARM TrustZone technology and a dedicated cryptographic security co-processor, aligning to the increased need for networked, secure systems. "Hierofalcon" is expected to be sampling in the second quarter of 2014 with production in the second half of the year.

"Bald Eagle" is the next generation high-performance x86-based embedded processor available as both an APU and CPU featuring up to four new "Steamroller" CPU cores within a 35W TDP. The APU products will provide the new power-optimized AMD Radeon Graphics Core Next GPU architecture and HSA enhancements for high-performance embedded applications, making it a superior solution for next-generation digital signage and embedded digital gaming. The "Bald Eagle" family will also introduce new power management features, such as configurable TDP, allowing engineers more design flexibility. "Bald Eagle" is expected to be available in the first half of 2014.

"Steppe Eagle" will further extend the performance and low-power range of the AMD Embedded G-Series APU SoC platform with an enhanced "Jaguar" CPU core architecture and AMD Graphics Core Next GPU architecture that include new features for increased CPU and GPU frequency. Designed for low-power embedded applications, "Steppe Eagle" is designed to offer increased performance-per-watt both at a lower TDP than the current AMD Embedded G-Series APU SoC, as well as extending the high-end performance above 2 GHz. "Steppe Eagle" also provides embedded design engineers the flexibility to leverage the current AMD Embedded G-Series APU SoC board design and software stack for a variety of applications with footprint compatibility. "Steppe Eagle" is expected to be available in the first half of 2014.

"Adelaar" is the next-generation discrete AMD Embedded Radeon GPU based on Graphics Core Next architecture specifically designed for embedded applications. Bringing industry-leading performance to embedded applications, "Adelaar" comes as a multi-chip module (MCM) with pre-qualified and integrated 2 GB of graphics memory. The "Adelaar" GPU family will deliver 3D graphics, multi-display support and support for DirectX 11.1, OpenGL 4.2 and both Windows and Linux. "Adelaar" is ex-

pected to be available in the first half of 2014 with seven years of planned supply availability as an MCM, mobile PCI express module (MXM) and standard PC graphics card.

AMD
www.amd.com

Agilent Technologies splits measurement from life-sciences businesses

The name "Agilent" is set to disappear from the front panels of test and measurement products – just as the logo "Hewlett Packard" did in a previous company split. When the computing products arm of the original Hewlett Packard outgrew the company's original measurement business, The T&M, medical, life sciences, analytics, optoelectronics and components business was separated off to become Agilent; a further fragmentation created Avago Technologies as an independent component company. Now, the electronic measurement portion of the business will once again become a separate entity. Agilent Technologies has announced plans to separate into two publicly traded companies: one in life sciences, diagnostics and applied markets (LDA) that will retain the Agilent name, and the other that will be comprised of Agilent's current portfolio of electronic measurement (EM) products.

The company's statement says that the two publicly-traded companies will offer shareholders distinct opportunities with unique investment identities; a \$3.9 billion-turnover life sciences, diagnostics, applied markets company, that will retain the Agilent name; and a \$2.9 billion-turnover electronic measurement company, to be named later. The "Transaction leverages strategic and operational advancements and improvements of both businesses," and the move "Allows management to focus exclusively on the customers of their respective companies."

"Agilent has evolved into two distinct investment and business opportunities, and we are creating two separate and strategically focused enterprises to allow each to maximise its growth and success," said William (Bill) Sullivan, Agilent president and CEO. "Agilent's history is one of reinvention, starting with our own separation from HP and including four major spinoffs since 2005. We are once again making a bold move, as we have done many times in the past, to ensure a future of sustainable growth for both the LDA and EM companies," he said. "We are focused on making this transition seamless for our customers."

The new EM company will be, "the world's premier electronic measurement company, with a leading position in major markets including communications; aerospace and defense; and industrial, computers and semiconductors." FY13 estimated revenues are \$2.9 billion. Ron Nersesian, who has been Agilent's president and chief operating officer, is executive vice president of Agilent and president and CEO-designate of the new EM company, effective immediately. Neil Dougherty, who has been Agilent's vice president and treasurer, is vice president of Agilent and CFO-designate of the new EM company.

More on the new **Agilent** and the new **T&M company**.

IMPROVED NOISE USING AN ACTIVE MATCH FOR A WIDEBAND FULLY DIFFERENTIAL AMPLIFIER

Since its first appearance in 1999, the single-to-differential configuration of wideband fully differential amplifiers (FDAs) have used a resistor to ground as part of the input match, at the cost of higher input referred noise voltage. If that resistor could be removed, with an input impedance match set solely by the path into the summing junction, a much lower input referred noise should be possible.

Removing the resistor would be a viable option when the input match can be maintained to very high frequencies via a common mode loop bandwidth of greater than 1GHz. The design equations for both approaches will be shown here with a comparison of input referred noise parametric on target gain developed.

SINGLE TO DIFFERENTIAL CONVERSIONS USING A FDA

One of the more useful functions supported by the growing range of FDA amplifiers is to convert from a single ended source to the differential output required by all modern ADC inputs. These can be either DC or AC coupled designs. When DC coupled, a careful attention to input common mode range is required and bipolar supplies can be useful, in that case, for many FDAs. For higher speed requirements, single supply is more common and an input match to some source impedance is often desired to limit reflections and/or SFDR degradation. While single supply FDAs can provide a DC coupled path, an AC coupled approach will be shown here to remove input common mode range considerations from this development. These same results will apply to a DC coupled design as long as the inputs stay in range. A typical AC coupled implementation of a doubly-terminated 50Ω input design is shown in Figure 1. This is targeting an example design set to a gain of 5V/V starting with a 499Ω feedback element and using a free Spice simulator to generate the schematic (Reference 1).

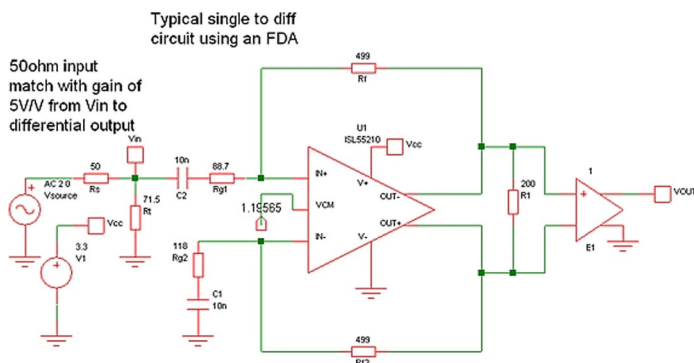


Figure 1. Gain of 5 V/V (14 dB), 50Ω input impedance, AC coupled, Single to Differential Design.

Several considerations are common to this type of circuit;

1. The feedback resistors are equal.
2. The input impedance is set as a combination of Rt and the impedance looking towards Rg1.
3. The impedance looking towards Rg1 will be increased

over just the Rg1 value by the action of the common mode loop within the FDA (Reference 2). That loop acts to hold the output common mode voltage fixed which will then cause the input common mode voltages to move with the input signal increasing the apparent input impedance looking into Rg1.

4. The Rg2 resistor is set to get differential balance as $R_{g1} + R_{t||R_s}$
5. With Rg2 set, the noise gain (NG) for this circuit is $1 + R_f/R_{g2}$.
6. With the AC coupling on the input paths, the DC I/O operating voltages default to the internally developed Vcm reference (1.2V for this 3.3V, single-supply device). That Vcm controls the output common mode voltage but, since there is no DC current path back to the input, it will also set the DC input common mode operating voltage.

The particular example above is using a very low noise, 4GHz gain bandwidth, FDA – the ISL55210 – where, in this case, the design started by selecting an Rf value then proceeded to solve for the Rt and Rg1 elements. There has been very little vendor guidance in splitting that input match contribution between the Rt and Rg1 elements. The tradeoff is that driving the Rg1 element down (Rt up) will reduce the input noise and extend the bandwidth (for voltage feedback based FDAs). Going in that direction depends more on the common mode loop bandwidth to set the input match into the Rg1 path (Reference 2). While most reported approaches to deriving the resistor values for the circuit of Figure 1 have either been iterative or approximate, picking an Rf for a target gain (Av) and input impedance (Rs) can be manipulated into a quadratic solution for Rt (ref. 3).

$$R_t^2 - R_t * \frac{2R_f(2R_f + \frac{R_s}{2} A_v^2)}{2R_f(2 + A_v) - R_s A_v(4 + A_v)} - \frac{2R_f R_s^2 A_v}{2R_f(2 + A_v) - R_s A_v(4 + A_v)} = 0 \quad \text{Equation 1}$$

Solving the coefficient denominator for zero will give a minimum Rf to send Rt to infinity depending then only on the Rg1 input path for the match. For the example here, this solves to 160.71Ω.

$$R_{fmin} = \frac{R_s A_v (4 + A_v)}{2(2 + A_v)} \quad \text{Equation 2}$$

As the Rf is reduced towards this Rfmin, the Rg elements will decrease while Rt will $\rightarrow \infty$. Using eq. 1 to get Rt as a decreasing Rf is selected, then the 2 other resistors are set by these expressions –

$$R_{g1} = \frac{2 \frac{R_f}{A_v} - R_t}{1 + \frac{R_s}{R_t}} \quad \text{Equation 3}$$

$$R_{g2} = \frac{2 \frac{R_f}{A_v}}{1 + \frac{R_s}{R_t}} \quad \text{Equation 4}$$

NOISE ANALYSIS FOR THE SINGLE TO DIFFERENTIAL FDA

Once a set of resistor values is determined using these design equations, they can be placed into a noise analysis circuit to arrive at a total output differential spot noise. All of the elements contribute to the noise as shown in the circuit of Figure 2 where the noise terms are shown as spot noise voltages and currents.

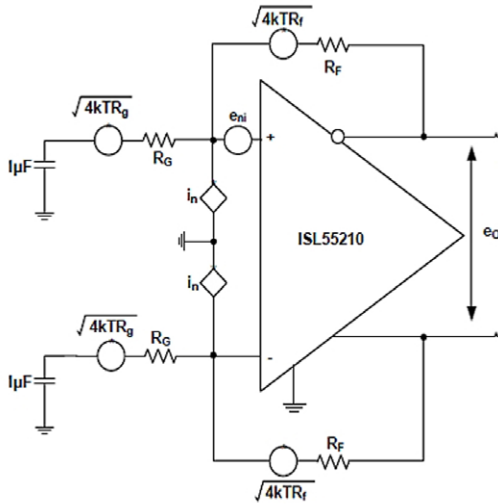


Figure 2. Noise analysis circuit for the FDA

For the situation here where the Rf and Rg elements are equal, and the current noise terms are equal, the total output noise expression is very simple as shown in Equation 5 where NG is the Noise Gain equal to 1+Rf/Rg. (page 14 of the ISL55210 data sheet).

$$e_o = \sqrt{(e_{ni}NG)^2 + 2(i_nR_f)^2 + 2(4kTR_fNG)} \quad \text{Equation 5}$$

Any wideband, voltage-feedback based FDA can use this design flow to move the implementation resistor values down to the minimum set allowed by Equation 2. Table 1 shows some of the lowest noise wideband FDAs to apply to this analysis.

FDA parts	Eni (nV/√Hz)	In (pA/√Hz)	GBP (Mhz)
ISL55210	0.85	5.00	4000
LTC6406	1.60	2.50	3000
ADA4930	1.20	3.00	2800
LTC6409	1.10	8.80	10000

Table 1. Some modern FDAs and key parameters. X

Stepping the Rf down for the example design of Figure 1, re-computing the other resistor values, and then the input referred noise, gives the results of Table 2. The resistor values (exact here) would be the same for any of these four example devices to give a gain of 5V/V from the input of Rt with a 50Ω input match (Reference 4). Input referring the output noise from Equation 5 by a gain of 5 gives the estimated input spot noise for each device in Table 2 (where these are still including the assumed 50Ω source noise collapsed into the Rg elements of Figure 2).

Rf	Rt	Rg1	Rg2	NG	ISL55210	LTC6406	ADA4930	LTC6409
500.00	71.18	88.11	117.48	5.26	2.16E-09	2.51E-09	2.27E-09	2.50E-09
462.31	73.79	80.43	110.23	5.19	2.07E-09	2.44E-09	2.19E-09	2.39E-09
424.63	77.14	72.72	103.06	5.12	1.98E-09	2.36E-09	2.10E-09	2.27E-09
386.94	81.60	64.97	95.97	5.03	1.88E-09	2.27E-09	2.01E-09	2.16E-09
349.25	87.81	57.16	89.02	4.92	1.77E-09	2.18E-09	1.92E-09	2.03E-09
311.56	97.09	49.26	82.26	4.79	1.66E-09	2.07E-09	1.82E-09	1.90E-09
273.88	112.46	41.22	75.83	4.61	1.54E-09	1.96E-09	1.70E-09	1.76E-09
236.19	142.95	32.95	69.99	4.37	1.41E-09	1.82E-09	1.57E-09	1.61E-09
198.50	233.38	24.21	65.39	4.04	1.25E-09	1.65E-09	1.41E-09	1.43E-09
160.81	67658.77	14.32	64.28	3.50	1.06E-09	1.41E-09	1.20E-09	1.21E-09

Table 2. Swept table of resistor values and resulting noise.

Decreasing the Rf design value will monotonically reduce the noise due to both decreasing resistor noise contributions and decreasing NG. The minimum value of 160.71Ω moves Rt to infinity giving the lowest possible input noise and noise gain. The decreasing NG (=1+Av/2 when Rt is open) will also extend the bandwidth for these voltage feedback devices. One tradeoff to moving these resistors down would be the ability of the common mode control loop bandwidth to hold the active input match over frequency, looking into Rg1, acceptably close to Rs. In the limit of Rt tending to ∞, that 14.3Ω Rg1 in the last row of Table 2 will be transformed into a 50Ω active input impedance by the common mode loop. Another concern might be the increased output stage loading due to lower Rf that will added to the actual differential load to possibly impair the harmonic distortion performance.

Plotting the input referred noise vs. Rf from Table 2 gives Figure 3. There is obviously a huge benefit in reducing the noise by reducing the Rf as far as is consistent with desired input match, frequency span and loading considerations. Starting from just picking Rf = 500Ω and proceeding down to the minimum 161Ω value for these design targets drops the total input spot noise from about 2.15 nV/√Hz to 1.06 nV/√Hz using the lowest noise ISL55210. Backing out the noise voltage delivered by the 50Ω source impedance to the matched input (that is still included in the 1.06 nV/√Hz minimum) gives an input referred noise for just the amplifier stage of 0.96 nV/√Hz.

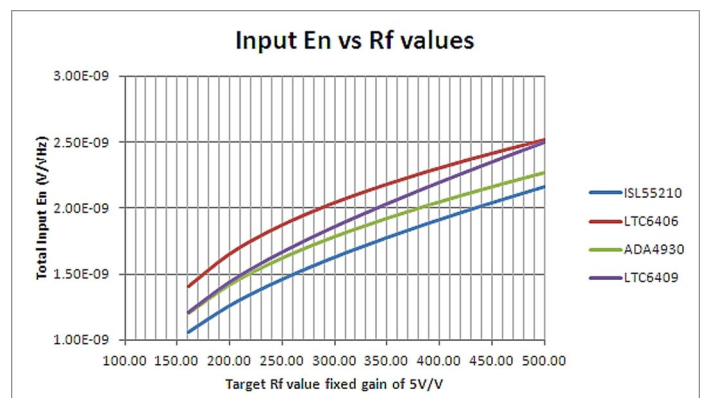


Figure 3. Input referred noise comparisons vs. target Rf value

ELIMINATING RT AND USING ONLY AN ACTIVE MATCH DESIGN

Taking this analysis to its limit, eliminating the Rt element to ground, uniquely solves for a set of required resistor values. Solving for the required Rf, given a target input impedance matched to Rs and a gain from Rg1 to the differential output, gives the simplified design equations 6 to 8 where eq. 6 is just the Rfmin expression of eq. 2 repeated.

IMPROVED NOISE USING AN ACTIVE MATCH

$$R_f = \frac{Av(Av+4)R_s}{2(Av+2)}$$

Equation 6

$$R_{s1} = \frac{R_s}{1 + \frac{Av}{2}}$$

Equation 7

And then, $R_{g2} = R_s + R_{g1}$

Eq. 8

Placing these expressions into the output noise calculation of Equation 5, using $NG=1+Av/2$ in this simplified design, and working into a Noise Figure (NF) expression, gives Equation 9 (Reference 5).

$$NF = 10 \log \left[2 + \frac{4}{A_v} + \frac{\left(e_{ni} \left(\frac{1}{2} + \frac{1}{A_v} \right) \right)^2 + \frac{1}{2} \left(i_{nr} R_s \frac{A_v + 4}{A_v + 2} \right)^2}{kTR_s} \right]$$

Equation 9

Starting from the gain of 14 dB (5V/V used earlier) and stepping the gain up in 2 dB steps for a fixed input impedance of 50Ω, and using the 0.85 nV/√Hz with 5 pA/√Hz current noise for the ISL55210 from Table 1, gives the required resistor values and resulting noise of Table 3.

Gain (dB)	Gain (Av)	Rf	Rg1	Rg2	Noise gain	Eo	Noise Figure
14	5.01	161.04	14.26	64.26	3.51	5.32E-09	7.51
16	6.31	195.71	12.03	62.03	4.15	6.36E-09	7.06
18	7.94	238.53	10.06	60.06	4.97	7.67E-09	6.68
20	10.00	291.67	8.33	58.33	6.00	9.30E-09	6.36
22	12.59	357.88	6.85	56.85	7.29	1.13E-08	6.08
24	15.85	440.62	5.60	55.60	8.92	1.39E-08	5.86
26	19.95	544.26	4.56	54.56	10.98	1.71E-08	5.67
28	25.12	674.28	3.69	53.69	13.56	2.12E-08	5.51
30	31.62	837.60	2.97	52.97	16.81	2.63E-08	5.39
32	39.81	1042.88	2.39	52.39	20.91	3.27E-08	5.28
34	50.12	1301.05	1.92	51.92	26.06	4.08E-08	5.20

Table 3. Swept Gain 50Ω active match element values and ISL55210 noise analysis.

This first row of values closely matches the earlier results in the last row of Table 2. These resistor values would be correct for any voltage feedback FDA while the output noise and Noise Figure are predicted using the ISL55210 input spot noise numbers. As is normally the case, increasing the gain will be reducing the input referred noise at the cost of reduced bandwidth as shown by the increasing noise gain (V/V). Continuing the gain of 5V/V design from Figure 1, but eliminating the Rt element and using the values in the first row of Table 3, gives the simulation circuit of Figure 4.

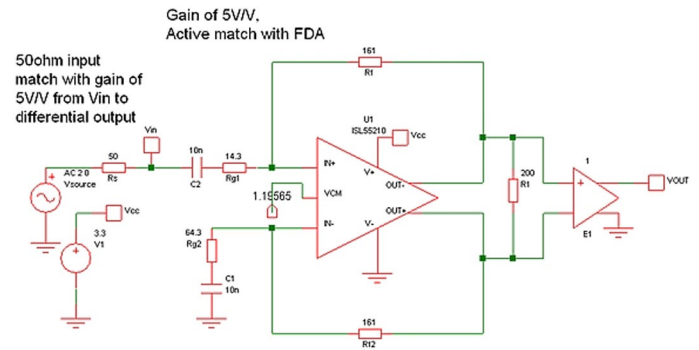


Figure 4. Gain of 5 V/V, 50Ω input, active match with wideband FDA.

With a noise gain =3.5 V/V in this circuit, this should give >1 GHz bandwidth for this 4 GHz gain-bandwidth device. While the simulations here are reasonably accurate, this circuit, over a wide range of gains and input impedances, can also be easily tested using the ISL55210-ABEV1Z Active Balun Evaluation Board.

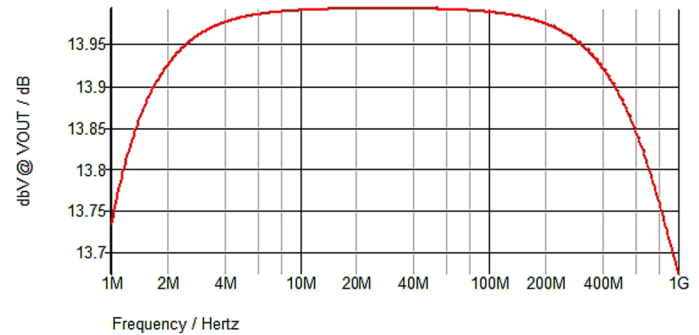


Figure 5. Frequency response shape for Vout/Vin from the simulation circuit of Figure 4.

Note the extremely fine scale on this simulation, showing <0.3 dB roll-off from 1 Mhz to 1 GHz where the low frequency roll-off is being set by the blocking capacitors. One final check is to look at the input impedance to see if, in fact, the common mode feedback loop is transforming that 14.3Ω Rg1 into something close to 50Ω. Changing the simulation circuit of Figure 4 to a current source input with a shunt 50Ω and probing the input voltage on an AC simulation should give close to 25Ω if the circuit is working correctly. Manipulating that data into just the impedance looking into Rg1 gives Figure 6. The simulated response closely matches the expected 50Ω with an increasing

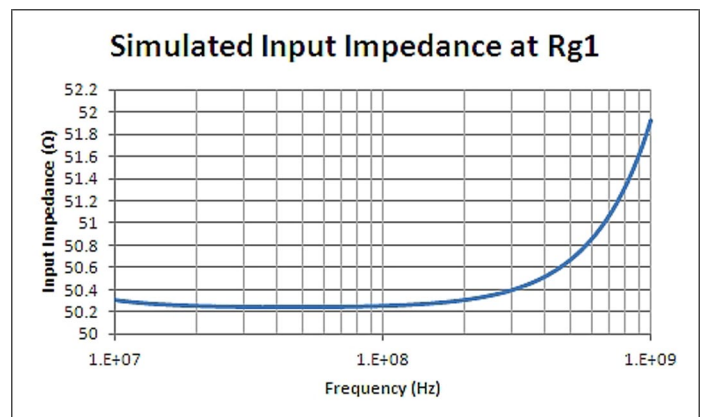


Figure 6. Input impedance for current source input to Figure 4.

impedance at higher frequencies as the common mode loop bandwidth rolls off. The match here exceeds 34 dB return loss through 1 GHz - far higher in frequency than previously available FDAs. This closely matches the measured input impedance for this circuit (Reference 6).

SUMMARY AND CONCLUSIONS

Wideband FDAs offer a useful circuit block for converting single to differential in high dynamic range signal processing designs. A closed form solution for the termination element to ground offers an easy means to assess tradeoffs in the split between that element and the series resistor into the summing junction. Increasing that R_t element decreases the other resistor values (for a fixed target input match and gain), which will then extend the bandwidth and reduce the noise. In the limit, removing R_t and depending only on the R_{g1} element and the common mode loop to set the input impedance will give the lowest noise and widest bandwidth response for any voltage feedback FDA. This application works best using FDAs with very high bandwidth common mode loops. This approach can potentially be used to replace an RF amplifier's single-ended-I/O-plus-balun solution with just this active balun configuration of the ISL55210. It has the added benefit over balun designs of isolating the load from the source impedance. The simple design equations shown here give considerable design flexibility in the input impedance and gain by changing just four resistors values.

REFERENCES:

- 1 . Intersil's free Spice and power simulator, iSim PE (registration required), <http://www.intersil.com/content/intersil/en/tools/isim.html>
- 2 . "Get a wideband matched input impedance with ultra-low noise using the active match capability of a new type of amplifier", Michael Steffes, <http://www.edn.com/design/analog/4410567/Wideband-matched-input-impedance-with-ultra-low-noise-using-the-active-match-capability-of-a-new-type-of-amplifier--part-1-of-2-->
- 3 . "DC-coupled, single-to-differential design solutions using fully differential amplifiers", Michael Steffes, http://www.planetanalog.com/document.asp?doc_id=528222&site=planetanalog
- 4 . These resistor values match those delivered by the ADI diff amp calculator - recognize the gain there is from the source and includes the divide by 2 to the input of R_t . <http://www.analog.com/en/amplifier-linear-tools/adi-diff-amp-calc/topic.html>
- 5 . Contact the author for the step by step derivation of this noise figure expression
- 6 . "Designer's Guide to the ISL55210-ABEVAL1Z Active Balun Evaluation Board", Michael Steffes, Intersil application note AN1831, <http://www.intersil.com/content/dam/Intersil/documents/an18/an1831.pdf>



Michael Steffes is Senior Applications Manager, High Speed Signal Path, at Intersil Corp.

technologies for cable processing and connectors

Highlight Segment 2013



productronica 2013

innovation all along the line

20th international trade fair for
innovative electronics production

messe münchen
november 12-15, 2013
www.productronica.com

UNDERSTANDING GROUNDING, SHIELDING, AND GUARDING IN HIGH IMPEDANCE APPLICATIONS

Inadequate shielding and bad grounding are often blamed when measurements are inaccurate, especially in high impedance applications. In fact, shielding and grounding problems are frequently responsible for measurement errors, but many test system developers aren't quite sure why. Many measurement errors can be traced back to currents from external fields that have become coupled into the measurement test leads.

This article explores how ground loops and poor or non-existent electrostatic shielding can cause error or noise currents to flow in measurement leads or the device under test (DUT), as well as techniques for identifying these error currents and preventing them from undermining measurement integrity. First, however, a review of electrostatics might provide a clearer understanding of the source of the problem.

REVIEW OF ELECTROSTATICS

Charges or charged particles are point sources of an electrostatic field (E-field). Field lines always emanate from the positive charge(s) and terminate on the negative charge(s). The force between charged particles is attractive when the charges on each particle are complementary and repulsive when the charges are identical. The E-field stores energy; the amount of energy stored is proportional to the total number of lines of flux (or to the total charge). The error current coupled into measurement conductors is directly proportional to the strength of the field. At any given voltage, the capacitance describes the relationship between charge and voltage on two conducting bodies. The energy stored in the field is equal to one-half of the capacitance multiplied by the square of the voltage: $E \text{ (Joules)} = \frac{1}{2}CV^2$. Wherever a voltage is present, there's also a distribution of positive and negative charges, even if one of the conductors is grounded.

Voltages generate a high impedance field. Currents (magnetic fields) generate a low impedance field. The field imped-

ance is always the ratio of the electric field to the magnetic field for any electromagnetic wave. Shields work by both reflection and absorption of field energy. If the terminating impedance of an electromagnetic wave is orthogonal to the wave impedance, reflection will predominate. If they are of similar impedance, absorption is the only possibility.

ELECTROSTATIC COUPLING

Charges unassociated with the measurement circuit are responsible for numerous measurement problems. If a charge is fixed in space around an unshielded measurement, the E-field from the charge will radiate to the measurement lead(s) and terminate on an image charge (a complementary charge of opposite polarity). Due to the E-field, a DC leakage current could potentially flow into the measurement leads. If a charge or a conductor with a charge distribution is moving in space with respect to the measurement circuit, an AC current ($I = V.dC/dt$, where C = the capacitance between the charge or the conductor and the measurement circuit) will flow into the measurement leads. External conductors at a different voltage than the measurement circuit behave in exactly the same way as point charges do. When the voltage on the external conductor changes, a current equal to $I = C.dv/dt$ will flow into the measurement. Both of these cases, i.e., point charges and differing voltages, will couple noise and error currents into the measurement. Any E-field line terminating on the measurement leads has the capacity to couple current into the circuit. E-fields dominate the interference landscape except when high currents are involved or whenever the instrument or measurement is operated near a transformer or a magnetic source. Ideally, all E-field lines from external sources should fall on a shield or guard instead of the measurement leads. Also, all E-field lines from the measurement and the instrument should fall on either the shield or the guard, never on outside conductors or charges. When the external E-field lines fall on either the shield or the guard, rather than the measurement leads, the measurement will be unaffected by these external electrostatic error sources.

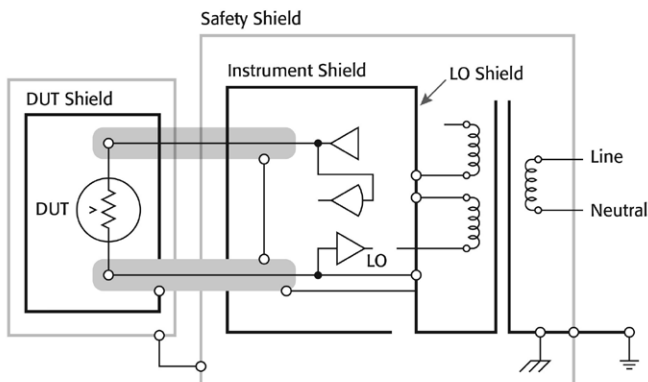


Figure 1. The proper use of the shield in a test system. The electrostatic shield is grounded to circuit common. Notice that both the HI and the LO terminals are shielded, and that the box surrounding the DUT provides a complete electrostatic shield.

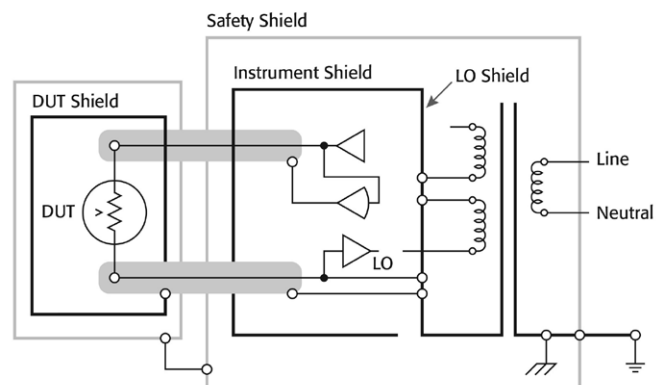


Figure 2. The proper use of the guard in a test system. Notice that both the HI and the LO terminals are either shielded or guarded, and that the box surrounding the DUT provides a complete electrostatic shield.

RF COUPLING

Radio frequency (RF) energy is ubiquitous. Any conductor of reasonable length, including the cables that connect instruments to devices, can act as an antenna for this energy. Although this radiation is outside the bandwidth of the source/measure instrumentation, the electromagnetic radiation will generate currents that travel up and down the antenna (in this case, the measurement leads). When these currents come in contact with the amplifiers inside the instrument, these currents may be rectified, causing a DC offset in the measurement. For this reason, both the HI and LO terminals require a shield to ensure that this current flows in the shield rather than in a measurement lead. The safety shield is usually used (outside the instrument common shield) as the shield for this source of noise. However, in order to provide complete shielding at these frequencies, the shield must not have any apertures (holes or slots) greater than $\lambda/2$, where λ is the wavelength of the interfering radiation.

MAGNETIC COUPLING

Magnetic coupling is unrelated to currents flowing in measurement leads but rather to the generation of voltages as predicted by Faraday's law of induction. The magnetic field (M-field), unlike the E-field, is a low impedance field. Conductors suitable for use as shields provide a matching impedance (unlike the high impedance E-field) to the M-field; as a result, they will not reflect the energy away from the measurement conductors inside. To shield an M-field, either the magnetic lines of flux must be diverted through a magnetic material (this works well at DC and low frequencies with μ -metal) or the shield must be thick enough to attenuate the field by absorbing the energy. To absorb the energy, the shield must be thick enough to attenuate the magnetic energy. For guidance on determining how thick the shield should be, I recommend Ron Schmitt's "Electromagnetics Explained: A Handbook for Wireless/ RF, EMC, and High-Speed Electronics" as a good reference.

SHIELDING

The purpose of shielding is to reduce or eliminate noise currents from coupling into electrical measurements. These currents can originate from point sources of charge, generating E-fields and voltage distributions. For example, people carry static charges with them wherever they go. AC line potentials in and around the laboratory or production environment can elicit AC E-fields, which, in turn, generate error currents. When devices under test are grounded outside the confines of the instrument, a different ground potential (different from the instrument) is responsible for yet another E-field generating current in the measurement ground lead. The isolation capacitance in the instrument's power transformer completes the circuit that supports the error current. Thunderstorms and environmental changes can cause electrostatic field changes. Radiation from RF sources can also generate currents in test leads, causing EMI rectified offsets in the amplifiers internal to the measurement instrumentation. Even in fair weather, the earth itself has a field with respect to the upper atmosphere of $\sim 100\text{V/m}$.

The electrostatic shield prevents external E-fields (a high impedance field) from affecting a measurement circuit by providing an equipotential surface to capture the E-field, deflecting it from the measurement leads inside. To prevent the shield from coupling internal circuits to one another, the shield ground point is connected to instrument LO inside the instrument. This

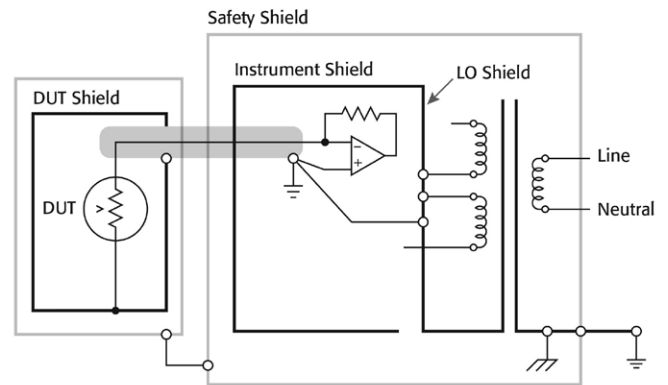


Figure 3. An illustration of the shield and guard configuration for an electrometer.

grounding scheme ensures that internal measurement nodes see only the instrument LO (Figure 1). To be effective, the shield must cover the entire measurement node. The instrument design should already include this shield wherever it is needed and provide for its extension to the outside world. Although this shield is a good idea for any measurement, it is imperative for high impedance measurements (i.e., any measurement $>100\text{ k}\Omega$). The resulting interference voltage is: $V = I_i \times R$, where I_i is the coupled current, and R is the impedance of the measurement. This shield does not prevent DC or AC currents from flowing between the measurement circuits and the shield. The common shield only provides protection from external electrostatic interference.

The driven guard accomplishes all that the common shield does, as well as eliminating the currents from the guard to the measurement circuits (Figure 2). The guard is simply a common shield buffered or driven to the measurement circuit voltage (instead of connected to instrument LO) to eliminate the E-field between the guard and the measurement circuit. Guards are used in circuits designed to measure or source very low currents, and are usually mandatory for currents of less than 1 nA . When measuring currents of 1 nA or less, the measurement node must first be guarded. Instruments used to measure or source these levels of current or lower will have the measurement guarded inside. It is not necessary to have a shield in addition to a guard around the measurement node, but the remaining measurement circuitry should be shielded. The

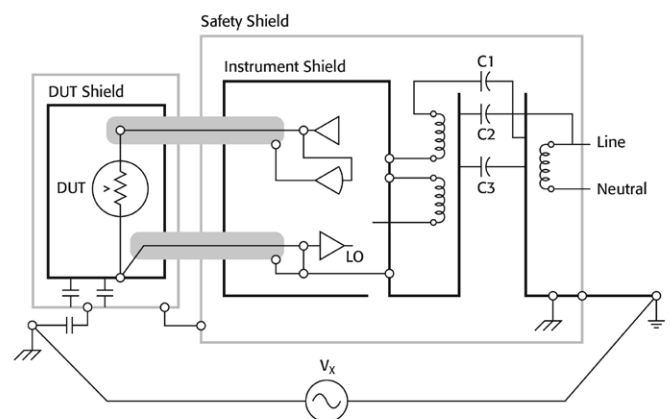


Figure 4. An illustration of the power system components that generate common mode current, as well as the isolation capacitances that support AC currents generated externally.

electrometer configuration allows a common shield to act as a guard as well, by ensuring that the measurement node is at ground potential (Figure 3).

This suggests that the fundamental difference between a shield and a guard is that a shield prevents external fields from affecting measurements, while a guard adds protection from DC leakage currents by surrounding the measurement node with a voltage identical that of the measurement node, both inside and outside the instrument, eliminating leakage currents.

SAFETY GROUNDING

The safety shield surrounds the electrostatic shield, protecting the instrument user from hazardous voltages on the DUT, or the measurement leads. The safety shield should be connected to earth ground at the instrument, and it should have a current capacity greater than the larger of the SMU output current and any earth referenced source driving the LO terminal. When this safety shield is in place, if a measurement lead, the electrostatic shield, or the driven guard was to touch the inside of the safety shield, the earth connection would keep the safety shield at a low potential. The safety shield also provides protection from the AC mains inside the instrument. In this case, the safety shield is the instrument chassis, which is also connected to earth. The safety grounding system follows the power system to allow this connection to be made. Instrumentation is safety grounded at the power inlet, ensuring that the metal instrument enclosure is always safe to touch. Even if a line voltage connection were to come loose and contact the enclosure from the inside of the instrument, the safety ground would keep the instrument chassis at a low potential and safe to touch.

The safety ground shield should never be used as the electrostatic shield. Even well designed instrumentation generates currents that travel down the safety ground in the line cord. Current from the power supply Y capacitors and higher frequency currents from a switching power supply can generate noise voltages on the instrument chassis with respect to external safety ground as the current flows through the inductance of the power line cord. The resulting noise voltage appears as a common mode voltage from the safety ground to the instrument chassis. This voltage is troublesome because instrumentation measurement common is not completely isolated from the in-

strument chassis (earth grounded). Every instrument generates some DC and AC leakage current across the instrument mains isolation barrier, and a finite capacitance from instrument common to the instrument safety ground. This capacitance is what facilitates the flow of AC current. We do not want these currents to flow through any part of the measurement pathway (Figure 4). These currents create voltage drops in the measurement leads, as well as voltages across other impedances in the measurement circuit. Because instruments may be designed to float hundreds of volts above earth ground, and shield ground should be connected to the instrument measurement common, the measurement terminals and electrostatic shield should always be considered unsafe.

GROUNDING THE SHIELD

Should the instrument shield (which is instrument LO) be connected to safety ground? Only if the application does not drive LO, and it should be done in a way that does not allow currents to flow in the measurement leads. From an instrumentation perspective, the only reason to connect LO to safety ground is to keep the measurement terminals within the common mode specification of the instrument. Given that the measurement LO terminal is floating in many instrument designs, a higher value (~100 kΩ) resistor can be added from safety ground to the measurement LO terminal.

COMMON MODE CURRENT

In the section titled “Safety Grounding,” I mentioned that the instrument(s) themselves are responsible for some of the current that generates the common mode voltage, V_x (Figure 4). These common mode currents are a direct result of the magnitude of the voltages on the primary and secondary windings of the power transformer acting on the unshielded capacitance across the transformer.

Figure 4 illustrates a typical instrument power transformer designed with primary and secondary shields. The shields within a power transformer perform the same function as the instrument shields already discussed. In the case of the instrument shield, when a portion of the measurement remains unshielded, external field lines can inject current into the measurement.

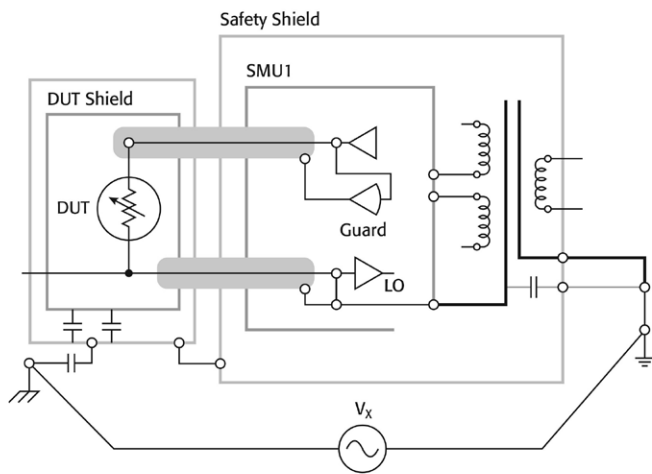


Figure 5a. With a single SMU, grounding the DUT, either directly or through a capacitance, can channel ground current into the measurement LO lead.

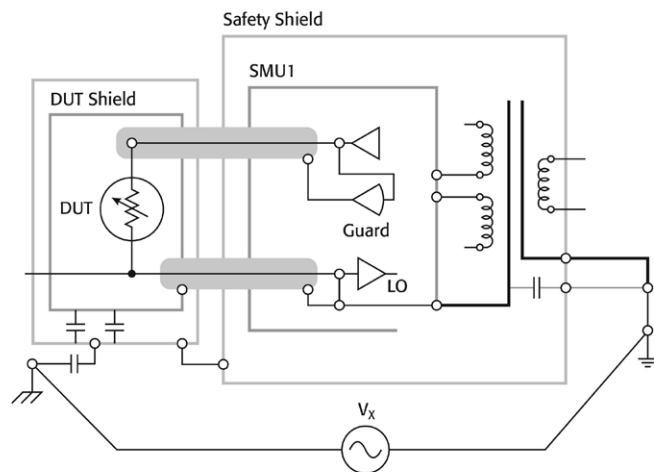


Figure 5b. In this single SMU application, grounding LO at the DUT, either directly or through a capacitance, leads to no error currents in the measurement LO lead.

The same is true with the power transformer, except due to the proximity of the primary to the secondary windings, as well as the magnitude of the voltages, the currents could be much higher if the transformer shields were absent. The capacitor C1 represents the unshielded capacitance from the secondary winding to the primary shield. This is the portion of the primary that remained unshielded. Likewise, the capacitor C2 represents the unshielded capacitance from the primary winding to the secondary shield. The total common mode current is the sum of the currents through each of these capacitors. The common mode current will increase as the primary and secondary transformer voltages increase or when the frequency of the power supply operation increases. The unshielded capacitance offers increasingly lower impedance to higher frequency edges, increasing the magnitude of the common mode current. Common mode current originating on the primary flows through the capacitor C2 into the secondary circuits, into the chassis through the measurement leads, and eventually returns to the primary ground that generated it. Common mode current originating on the secondary flows through the capacitor C1 into the primary circuit, into the chassis at the power entry module, then through the measurement leads, and eventually returns to the secondary ground that generated it. The net common mode current causes a voltage drop in the instrument power cord inductance, as well as a voltage drop in the ground connection between the DUT and the instrument. For this reason, it is best to use the chassis connection provided by the instrumentation whenever possible to avoid introducing a new safety ground to the system. The unshielded capacitance and, to a lesser degree, the DC resistance across the transformer can couple noise currents from other sources that generate differences in safety grounds throughout the building.

Consider a well-shielded and grounded single SMU test system; In the example shown in Figure 5a, if the measurement LO terminal were to be grounded to earth at the DUT LO terminal, either directly or through a capacitance, ground currents would flow in the measurement leads, and remote sensing would have to be used to eliminate the error voltage generated by the E-field between the two safety grounds. In Figure 5b, if the shield surrounding the DUT were connected to earth, current would not flow through the measurement LO connection. In this case, the capacitance from the DUT to its surrounding shield should be minimized. In Figure 5c, the shield is con-

nected to earth at the instrument through a current limiting resistor. In this case, the potential between safety earth grounds depicted by V_x does not force any current because only one safety earth ground has been introduced.

In all of these examples, the guard should be brought as close to the DUT as possible and dropped only after it is within the DUT shield.

Next; a well-shielded and grounded multi-instrument test system; Figure 5d introduces a second instrument into the test system. In this case, preventing all ground currents from entering into the measurement is difficult because there are two different safety ground connections. In this case, the resulting current can be reduced by connecting LO to safety earth with a high resistance at only a single point, by connecting both shields to the DUT shield, as shown in Figure 5d. In this case, the bulk of the current will flow through both power transformers and through the shield system. Some current will flow through the measurement leads, so remote sensing will also be necessary.

CONCLUSIONS

Most measurement errors can be traced to currents coupled into the DUT or into the measurement leads from external electrostatic (high impedance) fields. Adding an electrostatic shield properly grounded to the instrument LO can totally eliminate these noise sources. In some instances, a guard must be used instead of or in addition to an electrostatic shield, for very low current applications. Differences in the safety ground caused by safety ground currents generated from line-operated equipment can also cause measurement errors if the current is allowed to flow through the measurement leads. Common mode current from the test system's instruments contribute to these errors. The instrument power transformer supports this current so any connection to safety ground should be created as described. The safety shield used to maintain operator safety offers the added benefit of providing some low frequency RF shielding. If the instrument common is connected to safety ground with a relatively large resistor, the RF energy will not enter the instrument, and voltages due to EMI rectification can be minimized.

ABOUT THE AUTHOR

James Niemann is a Staff Engineer at Keithley Instruments, Cleveland, Ohio, which is part of Tektronix. He is responsible for designing instrumentation used in low-level measurements. He earned a Bachelor of Science degree in Electrical Engineering from the University of Akron. He has been awarded three patents for his work and has 24 years of experience in instrumentation design.

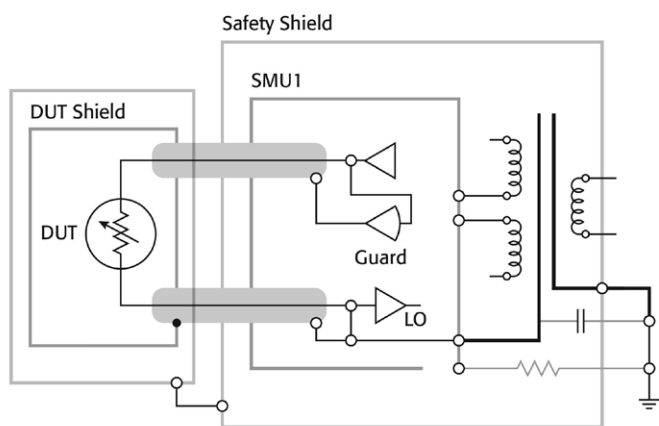


Figure 5c. With a single SMU, grounding the shield with a resistor, at the instrument leads to no error current in the measurement LO lead.

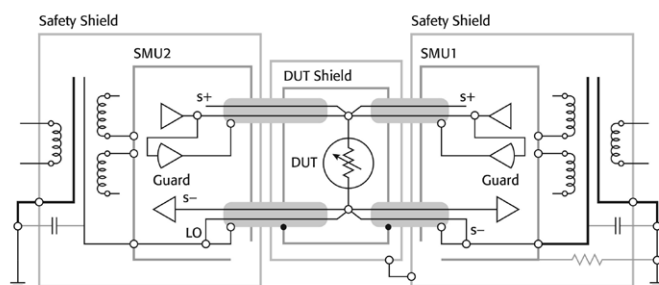


Figure 5d. With two SMUs, the remote sense lines compensate for the current flowing in the measurement leads generated from the use of two different grounds.



BY BONNIE BAKER

BAKER'S BEST



Rally your noise tools for a good offense

As they say in respect of all battles, the best line of defense is a strong offense. Whatever the task in hand, prepare to use every tool and weapon at your disposal. You never know what you might find and you want to be prepared! Applying an adequate amount of intensity to a project will earn you time so you can do what you enjoy most.

Apply this approach to tackling your ongoing circuit noise problems. Consider the noise in your new circuit design, and plan an organized campaign of action. The strongest tool that you will use is knowledge. With this knowledge in your tool box, you can smartly design a system where circuit noise is under control.

I choose to take this real-life, problem-solving technique into my electrical noise analysis activities. For instance, when I select an operational amplifier, I need to understand how much noise it will contribute to my system. From the electrical characteristic table in the product's data sheet, I scan the far right column (units), for the noise units such as $V/\sqrt{\text{Hz}}$, V_{rms} , or V_{pp} . You can see two of these units at the bottom of

Figure 1. Additionally, I scan through the typical performance curves looking for a y-axis title containing the word noise.

Let's first talk about the data sheet's electrical characteristic table. Input voltage noise density calls out a noise figure that refers to frequency with a bandwidth of one Hz. For instance, the electrical characteristics table in Figure 1 shows that the input voltage noise density at 10 kHz typically is equal to 17 $\text{nV}/\sqrt{\text{Hz}}$. Oh, did I mention that the input voltage noise density is a root-mean-square (rms) value (nasty assumption, not mentioned in the data sheet)? The rms noise value is equal to the mean of several samples from the amplifier at the test frequency plus one standard deviation.

The amplifier data sheet also contains a typical specification graph that shows the input voltage noise density versus frequency graphically. The top of Figure 1 shows the response of the OPA363 in this type of graph, where the input voltage noise at 10 kHz is approximately 17 $\text{nV}/\sqrt{\text{Hz}}$ (the same as the specification in the electrical characteristic table).

Now let's talk about the other specification. The input voltage noise specification is equal to 10 $\mu\text{V}_{\text{p-p}}$ across the frequency range of 0.1 Hz to 10 Hz. Note that the voltage noise density of the amplifier at 0.1 Hz and 10 Hz is approximately 3000 $\text{nV}/\sqrt{\text{Hz}}$ and 230 $\text{nV}/\sqrt{\text{Hz}}$, inclusive. You calculate the input voltage noise specification as the total noise in the area beneath these two frequencies. Since you are now analyzing the noise in a bandwidth, the denominator of the voltage noise density specifications cancel out.

But this is not the whole story. The units for input voltage noise specification are peak-to-peak volts instead of an rms value of $V/\sqrt{\text{Hz}}$. To convert an rms value to peak-to-peak, you simply multiply the rms value by 6.6. That is equal to twice the industry-standard crest factor (CF) of 3.3.

Now the question is how might you use this information to design your circuit? Stay tuned to hear the rest of the story in future posts.

REFERENCE

1 Baker, Bonnie, "Matching the noise performance of the operational amplifier to the ADC," Analog Applications Journal (slyt236), Texas Instruments, 2Q2006. www.ti.com/litv/pdf/slyt237

2 Trump, Bruce, "1/f Noise—the flickering candle," The Signal, Texas Instruments, March 03, 2013. http://www.edn-europe.com/en/1/f-noise-the-flickering-candle.html?cmp_id=34&news_id=10002485&vID=23

Bonnie Baker is a senior applications engineer at Texas Instruments and author of A Baker's Dozen: Real Analog Solutions for Digital Designers.

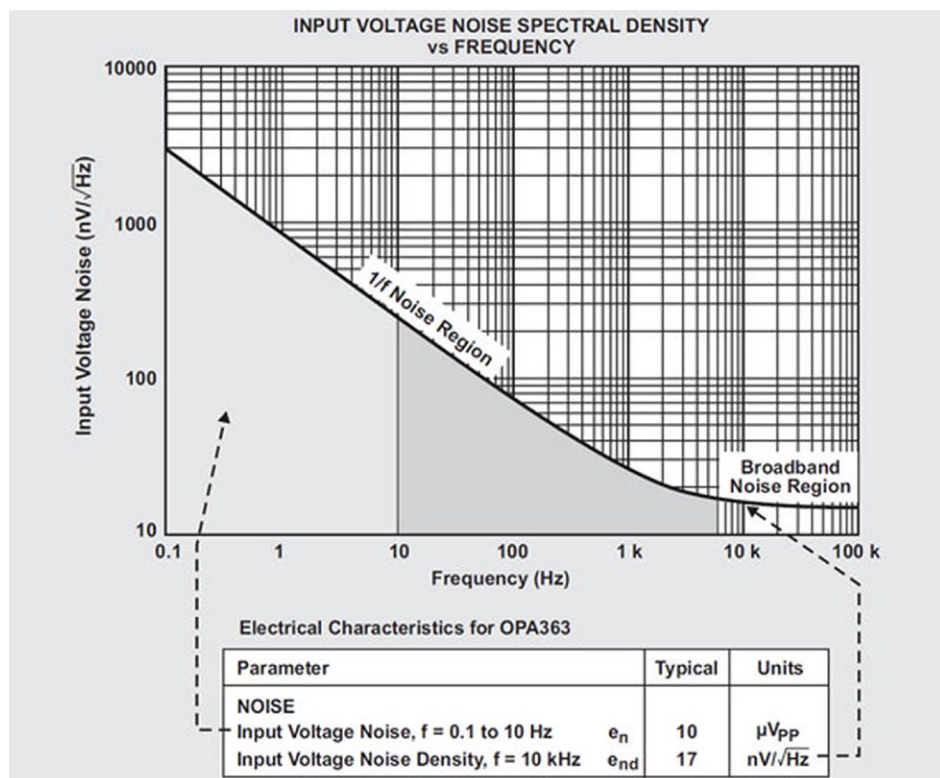


Figure 1. Amplifier product data sheet noise specifications for the OPA363.

Wireless temperature/humidity module

Fall is here, and that means heating season will soon arrive – or, depending where you are located, may already be here. If you have an acoustic guitar, you know that humidity – or lack thereof – is the enemy.

That's why I keep three plastic film canisters with sponges in my case to keep the humidity up. But the sponges dry out. Wouldn't it be nice to know when the sponges need more water without having to open the case?

That's where a wireless temperature/humidity logger can help. The WiFi-502 temperature/humidity logger from Measurement Computing has 802.11b WiFi and USB connectivity. Having an evaluation unit on hand, I decided to use it.

The Wifi-502 comes with a micro-USB cable, which you can use to perform initial setup once you download and install the EasyLog software. Installing the software and connecting to my XP laptop was a breeze. The installation needed Microsoft .NET Framework 2.0, which downloaded and installed automatically.

With the software installed, I connected the logger using the supplied micro-USB cable. The system found the new hardware and connected to it. A setup screen then appeared that let me select temperature units, set high and low alarms (for both temperature and humidity), and set a sample rate and number of samples per transmission from the logger to the host computer. The default is 10 seconds between samples and six samples per transmission to the host. Temperature range is -20°C to +70°C.

Once you establish a wired connection, you can set up a wireless connection to your local network and disconnect the cable. Once the wireless connection is established, you can configure the module without the USB cable, which becomes a charge cable only. (The cable works with an iPhone charger.) Figure 1 shows the logger and the initial PC screen, which includes a live image of the logger's display. You can run multiple loggers with one network.



Figure 2 shows the operating screen. The last transmitted temperature and humidity, the WiFi signal strength, and the state of the battery charge are visible. Having battery charge visible is a huge help. Other icons let you mute the audible alarm (for temperature and humidity) and return to the settings screen. To view and save data, click on the View Graph icon.

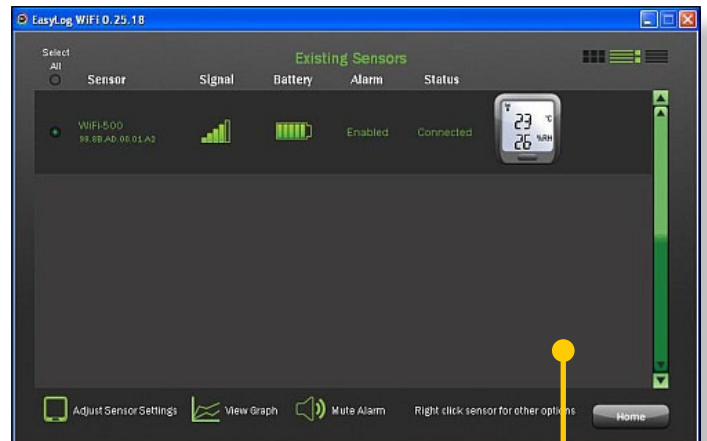


Figure 2 The operating screen shows the latest readings and it provides links to graphing and alarms.

When you click on the View Graph icon, another window opens that lets you select a date range for viewing. A list of date ranges let you select which range to view. The graph (Figure 3) has a vertical line that moves with your mouse. Under the graph, you see the temperature and humidity at the selected time. You can save the data in a text file for later use. If you export the data, Excel will automatically open and you'll get two sheets, one with a graph and one with the raw data.

Figure 1 A networked temperature and humidity logger transmits data to a computer on the network. The difference in temperature between the logger and the computer occurred because the logger doesn't transmit in real time.

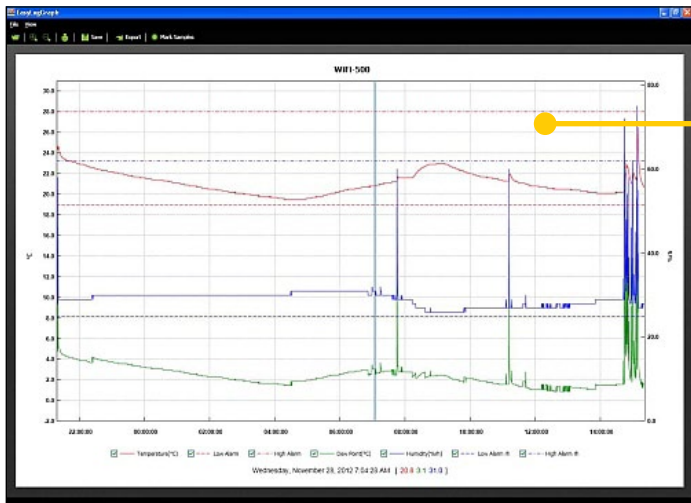


Figure 3 The graphing screen lets you find the temperature and humidity at any point in time.

A 14-lead flexible printed cable connects the motherboard to the display. The micro-USB receptacle is on the left. The micro-controller is an STM32L152R8T6 from STMicroelectronics.

OPEN IT

Having shown that the WiFi-502 module works, I opened it using an Allen wrench. See Figure 4. The module uses a GainSpan GS1011MIPS WiFi interface, which provides 802.11b wireless connectivity (see Figure 5). The GainSpan board mounts to the motherboard and includes the etched copper antenna (looks like a square wave).



Figure 5 The Wifi adapter module mounts to the logger's main board.

Note the connector in the lower left. It connects to a 4-lead ribbon cable that goes to a sensor attached to the back cover. That's the humidity sensor assembly. It's quite sensitive as the measured humidity rises quickly when you place the logger in your hand.

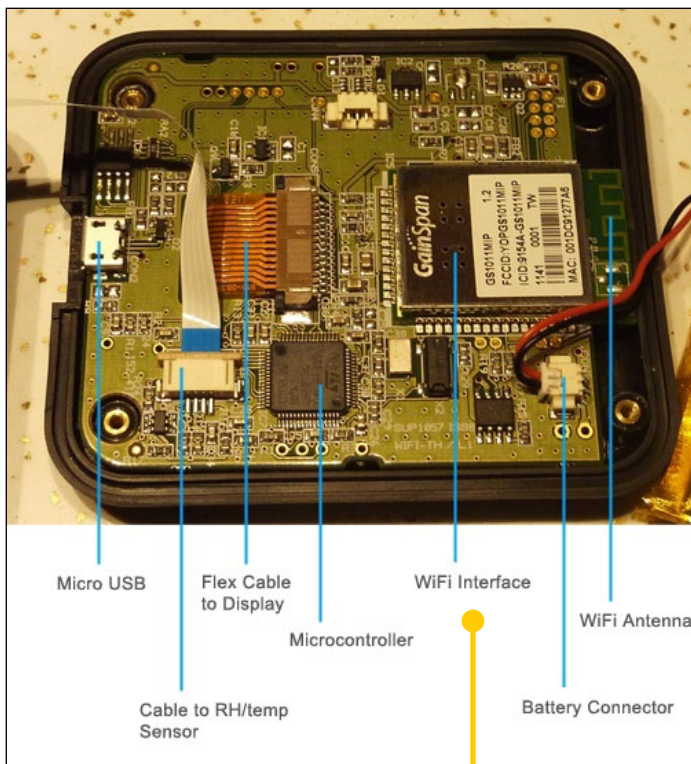


Figure 4 Inside the logger is the Wifi adapter, microcontroller, and connections to the battery and sensors.



Keep abreast of the latest industry news with our newsletters



www.electronics-eetimes.com/newsletters

AUTOMOTIVE SAFETY AND ISO 26262 QUALIFICATION OF COMPILERS

Microcontroller usage within the automotive industry is widespread with 32-bit devices found in everything from comfort controls, stability and traction control systems through to engine management. Software complexity in automotive electronic control units has also been increasing steadily and has created the need to provide a number of standards frameworks to ensure software code reliability and functional safety.

For functional safety in industrial equipment, IEC 61508 has been the widely required risk-based safety standard, where the risk of hazardous operational situations is qualitatively assessed and safety measures are defined to avoid systematic failures. Designed to bring about a similar degree of confidence for automotive applications, ISO 26262 is the automotive-specific standard based on IEC 61508. The ISO 26262 standard addresses the specific needs of automotive electric/electronic systems used in mass-produced passenger road vehicles with a maximum weight of 3.5 tons. Chapter 11 of part 8 of the ISO 26262 standard is designed to specifically address the use of software tools in the development of automotive systems and their potential impact on safety.

The principle behind this part of ISO 26262 is to ensure that all potential errors related to the tools used in the software development process can be avoided or detected. To do this, ISO 26262 requires that developers determine a Tool Confidence Level (TCL) consistent with the way the tool is applied. Depending on the desired Automotive Security Integrity Level (ASIL), ISO 26262 recommends qualification methods for a given TCL. A high TCL requires an intensive qualification method (e.g. a validation suite), while TCL1 (the lowest TCL rating) requires no qualification method for the tool. However, achieving a low TCL requires the detection of potential errors of the tool in the application process, which in turn may involve more effort in integrating the error checks and restrictions into the development process.

ISO 26262 is based on the idea of safety goals. Different goals are specified for each automobile system, such as an airbag system (ISO 26262 distinguishes between 'elements', 'items' and 'systems'). The corresponding ASIL is determined for the system. Level A represents the least stringent safety measure for avoiding an unreasonable residual risk, and level D is the most stringent.

In the context of ISO 26262, a software tool simplifies or automates activities and tasks required for the development of a safety-related system. ISO 26262 requires that all tools be considered independent whether they are in-house, freeware or commercial. The overall objective of tool qualification is to provide evidence that the tool is suitable to develop a safety-related system in such a way that one can ensure confidence in the correct execution of the tool.

To establish that confidence, ISO 26262 asks two questions and derives a well-defined confidence level from the answers. The first question deals with tool impact: Does a malfunctioning software tool and its potentially erroneous output lead to the violation of any safety requirement allocated to the safety-related system being developed? If the answer is 'no', the tool is classified as T11 (zero tool impact). If the answer is 'yes' (tool categorised as T12), a second question asks about the probability of detecting or preventing tool errors in the output of the software tool. Probability in the context of tool qualification denotes a qualitative measure and not a concrete number.

- TD1 indicates a high degree of confidence that a malfunction or an erroneous output from the software tool will be prevented or detected.
- TD2 indicates a medium degree of confidence that a malfunction or an erroneous output from the software tool will be prevented or detected.
- TD3 applies to all other cases.

Finally, the TCL is derived from the TI (Tool Impact) and TD (Tool Error Detection), as shown in Table 1.

	TD1	TD2	TD3
T11	TCL1	TCL1	TCL1
T12	TCL1	TCL2	TCL3

Table 1: Calculation of TCL by TI and TD, according to ISO 26262, Part 8, Section 11

The TCL describes the confidence the user should have in the tool and what actions need to be taken in order to ensure safety when using the tool. Tool providers have the chance to sell qualification kits that allow users of their tools to document the qualification process and determination of TCL based on their specific usage scenarios. Once the TCL is determined, a qualification method is chosen, if necessary.

Each qualification method is derived from two inputs: the ASIL of the safety-related system (documented in ISO 26262 "safety plan") and the determined TCL.

There are four different qualification methods proposed in the standard:

- Increased confidence from use
- Evaluation of the tool development process
- Validation of the software tool
- Development in compliance with a safety standard

The standard also provides individual chapters for the first three qualification methods. These chapters include a definition of terms, criteria, and instructions needed for a tool qualification (see ISO 26262, part 8, sections 11.4.7–11.4.9).

A tool rated TCL1 does not need any further qualification independent of the ASIL because it has either no influence on the safety functions; or its potential errors are detected with a high level of probability. For TCL2 and TCL3 (and depending on the ASIL), the software tool must also be qualified according to the methods shown in Tables 2 and 3. For a given ASIL, one qualification method marked with “++” (highly recommended) must be applied. Methods highly recommended for higher ASILs can also be used for lower ASILs.

Methods	ASIL			
	A	B	C	D
1a Increased confidence from use	++	++	++	+
1b Evaluation of the tool development process	++	++	++	+
1c Validation of the software tool	+	+	+	++
1d Development in compliance with a safety standard	+	+	+	++

Table 2: Qualification Methods for a Software Tool Classified as TCL2.

Methods	ASIL			
	A	B	C	D
1a Increased confidence from use	++	++	+	+
1b Evaluation of the tool development process	++	++	+	+
1c Validation of the software tool	+	+	++	++
1d Development in compliance with a safety standard	+	+	++	++

Table 3: Qualification Methods of a Software Tool Classified as TCL3.

In some cases a particular qualification is not possible, is too costly or not desired. For example, it could be quite costly for a company to set up and run an entire test suite to qualify a compiler. In these kinds of circumstances, augmenting the development and testing process can reduce the TCL. However, this can only be achieved by extending the development process with additional checks to discover or prevent the potential errors. In some cases, these extensions can be done using extra checking tools, such as a MISRA C code checker or some type of static code analysis. In other cases, the extension to reduce the TCL requires enhanced application testing or manual steps such as reviews. In most cases, the process extensions also require additional efforts and costs. Ultimately, development teams need to consider the cost of the enhanced process.

The value of a qualified tool with a high TCL depends on the costs of the alternatives in the process and the frequency the process is applied. For example, if a tool is applied every day and a review of its output is required to reduce the TCL to TCL1, the review costs could be quite high; tool qualification is much cheaper, even under the previously mentioned restrictions of the applicable tool qualification methods.

Wind River has collaborated with Validas AG, a software engineering firm in the field of safety-based systems that offers certification support according to ISO 26262, IEC 61508 and DO-178B, to develop the Wind River Diab Compiler. Together the companies have created a qualification kit for the Diab

Compiler where a high TCL can be justified. This qualification method should be applied if the effort related to error detection for each application of the tool in a given period is higher than the costs of the required tool qualification. The costs of tool qualification, which are constant for a given version, pay off during the repeated application of the qualified tool. The application of a qualified tool saves costs compared with a non-qualified tool.

When approaching tool qualification according to ISO 26262, the first consideration with respect to the TCL is the compiler and the linker. Table 4 is an example of a partial list of errors and checks that would impact TI and TD. It is based on the process of performing a compilation and linking of a given piece of C code using a makefile-based build process. The example aims to illustrate the concept of evaluating the error risk related to TI and the checks that help detect the errors (related to TD). It is not intended to show all possible existing errors in such a tool chain.

Item	Tool	Error / Check (Probability)	Error Description	Tool-Error-Detection
1	Compiler	Error	Cuts long function names	TD2
2	Make	Error	Missed dependency	TD1
3	Compiler	Check (high)	Finds syntax errors in C-code	
4	Linker	Check (medium)	Find truncated function names	
5	Review	Check (high)	Finds overlooked dependencies	

Table 4: List of Assumed Errors and Checks

Tool classification and qualification are important parts of the ISO 26262 standard. They can determine the level of effort that a company will have to spend on qualifying a particular tool based on the risk the tool has of introducing errors and the ability of the tool or the user’s development process to check and catch these errors. ISO 26262 is very flexible and allows different methods of tool qualification based on the required ASIL level and the Tools Confidence Level determined during the classification process. A vendor-supplied qualification kit is a significant option for qualifying a compiler according to ISO 26262 and will help guide the user through the complex qualification process. The savings in time and effort from the use of these qualification kits can be significant.

Graham Morphew is Director, Product Management, Tools & Lifecycle Solutions, at Wind River; www.windriver.com

**Automotive
Electronics**

EE Times
europe
AUTOMOTIVE

www.automotive-eetimes.com

10 C LANGUAGE TIPS FOR HARDWARE ENGINEERS

It can be common for a hardware designer to write code to test that hardware is working. These 10 tips for C—still the language of choice—may help the designer avoid basic mistakes that can lead to bugs and maintenance nightmares.

On its own, the software-development process has numerous hazards and obstacles that require navigation in order to successfully launch a product. The last thing that any engineer wants is challenges resulting from the language or tool that is being used. It often makes sense or is necessary for the hardware designer to write code to test that the hardware is working or, in resource-constrained cases, develop both hardware and embedded software. The language of choice is still C, and despite the advances in tools and structured programming, time and again basic mistakes occur that lead to bugs and maintenance nightmares. In an attempt to avoid these C-programming pitfalls, here are 10 C language tips for hardware engineers.

TIP #1: DON'T USE "GOTO" STATEMENTS

A couple decades or so ago, when computer programming was in its infancy, a program's flow was controlled by "goto" statements. These statements allowed a programmer to break the current line of code and literally go to a different section of code. Listing 1 shows a simple example. Programming languages eventually began to incorporate the idea of a function, which allows the program to break off to a section of code. Rather than requiring another goto statement, however, when completed the function returns to the next instruction after the function call. Listing 2 shows an example. The result was improved program structure and readability, and ever since, this has been considered the appropriate way to write a program. The very sight or thought of goto statements can cause software engineers to cringe and shudder in distaste.

LISTING 1 USE OF A GOTO STATEMENT

```
void main(void)
{
    int Count = 0;

    // Do Something

    // Wait for a while
    WAIT:
    if (Count < 5000)
    {
        goto WAIT;
    }

    // Do more stuff
}
```

One of the main reasons is that a program with goto's sprinkled throughout is very difficult to follow, understand, and maintain.

TIP #2: USE FOR(;;) OR WHILE(1)

If goto's are out, some hardware engineers may wonder how an infinite loop can be created for the program. After all, this may have been done before by creating a goto statement that returns to the top of main. The answer is to take advantage of the looping statements that are already built into the C language: for and while (listings 3 and 4).

The loop conditionals in the listings are relatively straightforward. The for loop is nothing more than the for conditional with no conditions. The while loop, on the other hand, will execute as long as the statement is true, which is the same as having any nonzero value for the condition.

TIP #3: USE THE APPROPRIATE CONDITIONAL STATEMENT FOR THE JOB

Program execution time can be highly dependent on the type of conditional structure that is selected for making a decision, in addition to the readability of the code. Many hardware engineers are familiar with the use of the simple if statement. Sometimes, however, the engineer doesn't realize that if the first condition isn't correct, an else or else if statement can be used. This can save the processor time by not having to evaluate another conditional statement. In the before code in the example shown in Listing 5, if Var is equal to one, the code will still check to see if the Var is equal to zero. However, in the after code that uses the else, only the first statement is evaluated, and then the code moves on, thereby saving clock cycles and making the code more clear.

The if/else if/else statements still may not always be appropri-

LISTING 2 USE OF A FUNCTION

TO CONTROL FLOW

```
void main(void)
{
    // Do Something

    // Wait for while
    Delay (50);

    // Do more stuff
}
```

LISTING 3 USE OF AN INFINITE

FOR LOOP

```
// Using a for loop to create the
infinite program loop
void main(void)
{
    // Initialize the system
    Sys_Init();

    // Run the program forever
    for(;;)
    {
        // Run the cool application
    }
}
```

LISTING 4 USE OF AN INFINITE

WHILE LOOP

```
// Using a while loop to create the
infinite program loop
void main(void)
{
    // Initialize the system
    Sys_Init();

    // Run the program forever
    while(1)
    {
        // Run the cool application
    }
}
```

ate. If there are a number of possible conditions that need to be checked, a switch statement may be more appropriate. This allows the processor to evaluate the statement and then select from a list of answers what it should do next rather than continually evaluate a bunch of conditions. Listing 6 shows an example that corresponds to the same type of example shown in Listing 5.

The moral of the story is simply to keep alternative conditional-statement options open and select the most appropriate for the job. This approach will make it easier to understand the flow of the program by making the structure straightforward and could squeeze extra clock cycles out of the processor.

TIP #4: AVOID USING ASSEMBLY LANGUAGE

The natural language for a microprocessor is assembly language instructions. Writing a program in the low-level machine language can result in more efficient code for the processor. Humans, however, don't naturally speak this language, and as experience has shown, writing assembly language results in misunderstanding. Misunderstanding then leads to improper maintenance, or worse, and the result is a system overridden with

bugs. A general tip is to avoid the use of assembly language. The detailed truth of the matter is that most compilers now compile very efficient code. Developing in the higher languages, such as C/C++, results in a more organized structure, which is easier to understand and maintain, and produces overall better code. Listing 7 shows an example that compares the use of assembly and C code to increment a 32-bit variable. With that said, there are still occasions when it is appropriate to use assembly language, but those times are scarce. The first recommended time is when developing a boot-loader. In this instance, during start-up it may be necessary to optimize how quickly a decision is made to boot the application or the boot-loader. In this case, assembly code for the branch decision may make sense. Another case is when developing a control loop that has tight timing requirements on a DSP. In order to squeeze every clock cycle out of the device, it may make sense to code the control loop in assembly. If the task at hand is appropriate for using assembly, make sure that it is well documented so that future developers (or future versions of yourself) can understand what the code is doing.

TIP #5: TAKE ADVANTAGE OF MODULARITY

One of the most common experiences the author has when taking on a new project that was started by hardware engineers is the atrocious organization of the code. It isn't uncommon to find that code consists of a single main module with in excess of 25,000 lines. In these applications, everything is global, functions are sparse, and goto statements rule the organization of the code. This was the norm 15 years ago, but not anymore! Programming in C/C++ has given engineers the ability to break up their code into separate functional modules. This eases navigation of the code but also allows an engineer to use object-oriented techniques such as encapsulation. Where it makes sense, organize code into logical modules. It'll take a little bit more time up front (a few minutes), but in the long run it will save many long nights and debugging headaches!

TIP #6: WRITE LASAGNA NOT SPAGHETTI CODE

Beningo is an Italian name, and as with any good Italian, my love of pasta is a given. When comparing pasta with software, spaghetti and lasagna come to my mind. Spaghetti is chaotic; noodles intertwine, going this way and that way and resulting in a complete lack of any type of structure. Writing unstructured code is exactly like spaghetti: With each bite, you have no clue what you are going to get!

On the other hand, there is lasagna! The noodles are layered, giving the meal structure. Code developed using layers not only is easier to understand, it has the potential to have one layer re-

LISTING 5 USE OF IF/ELSE INSTEAD OF JUST IF

```
if(Var == 1U)
{
    // Do something neat
}
if(Var == 0U)
{
    // Do something cooler
}

if(Var == 1U)
{
    // Do something neat
}
else
{
    // Do something cooler
}
```

10 C LANGUAGE TIPS

LISTING 6 USE OF SWITCH STATEMENTS

```
switch (Var)
{
    case 1:
        // Do something neat

        break;

    case 0:
        // Do something cooler

        break;

    default:
        // Should never get here
        // Error or something

        break;
}
```

moved and a new layer added, basically allowing for reuse and ease in maintainability. Figure 1 shows an example of a simple software model that uses the lasagna model.

TIP #7: USE DESCRIPTIVE VARIABLE NAMES

One of the barriers to writing great software that is understandable and easy to maintain is the naming convention of variables. In an effort to keep variable names short, it is common for developers to create shortened, cryptic mnemonics that only they can understand once in a blue moon. Modern languages allow for hundreds of characters to be included in a variable name. To keep things clear, “call a spade a spade,” as the phrase goes, rather than something else. This will make the variable name obvious not only to the developer but also to future maintenance teams. Listing 8 shows an example.

TIP #8: USE #PRAGMA STATEMENTS SPARINGLY

In the C language, there is a special type of statement known as #pragma. These statements often handle nonstandard syntax and features. They should be avoided as much as possible because they are nonstandard and will not port from one pro-

LISTING 7 INCREMENTING A VARIABLE IN ASSEMBLY VERSUS C

<pre>INC [_Sys_Tick+3] JNZ .GoReturn</pre>	<pre>;Increment Byte LSB ;Jump is no overflow</pre>	<pre>Sys_Tick++;</pre>
<pre>INC [_Sys_Tick+2] JNZ .GoReturn</pre>	<pre>;Increment Byte 1 ;Jump is no overflow</pre>	
<pre>INC [_Sys_Tick+1] JNZ .GoReturn</pre>	<pre>;Increment Byte 2 ;Jump is no overflow</pre>	
<pre>INC [_Sys_Tick]</pre>	<pre>;Increment Byte MSB</pre>	
ASSEMBLY		C CODE

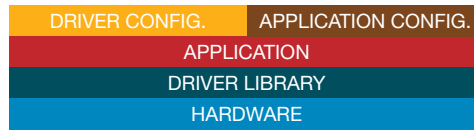


Figure 1 Code developed using layers is easier to understand, and it has the potential to have one layer removed and a new layer added, allowing for reuse and ease in maintainability.

LISTING 8 VARIABLE NAMING

```
int Frq;           int Frequency;
int Btn;           int Button;
int MtrState;     int MotorState;
int Spd;           int Speed;
```

cessor to the next. Some compilers may require them for tasks such as defining an interrupt service routine. In these instances, there may be no way around using a #pragma. If possible, keep all of the #pragma statements together in one module or in a couple of modules. This will help to ensure that when the code is ported, there are only a few places to update the code rather than areas sprinkled throughout the code base. This will also help prevent a nightmare when the ported code is compiled for the first time.

TIP #9: ERRORS AREN'T ALWAYS AS THEY SEEM

One of the gotchas to look out for when debugging a C program is compiler errors. Depending on the sophistication of the compiler, when an error is detected, more often than not the error lies somewhere in the program other than where the compiler is indicating. The reason for this has to do with the steps that the compiler takes to generate the program. The types of errors are generally consistent, so there are a few errors an engineer can look for that nine times out of 10 are the culprit:

- Watch for missing #include files. This can result in the developer looking at a perfectly good line of code, but because the necessary header files aren't included, the compiler flags it as an error, indicating that something is not defined.
- Watch for missing semicolons. One of the most common errors when writing C code is to forget the semicolon at the end of a statement.
- Watch for missing brackets. Brackets are another common mistake and are either left out by accident or because mistyping produces a different character.

- Watch for missing commas. In complex definitions, it's easy to forget the comma!

In general, when a strange compiler error pops up, look around at what might have been compiled immediately before that line. Odds are that is where the mistake is! It may be one line up, half a page away, or in a completely different file. Don't give up! With some experience, finding the difficult ones eventually becomes second nature.

Your Global Link to the Electronics World



www.electronics-eetimes.com



www.ledlighting-eetimes.com



www.microwave-eetimes.com



www.analog-eetimes.com

```

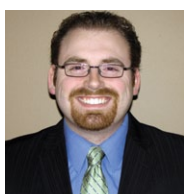
\
  int
  _,l;\
  char*I,
  *0[]={""",
  "gjstu","t"
  "fdpoe","uij"
  "se","gpvsui",\
  "gjgui","t"
  "jyui","tfwf"
  "oui","fjhui",
  "ojoui","ufoui",\
  "fmfwfoui","uxfmgui"
  "i","b!qbsusjehf!jo!"
  "b!qfbs!usff!\xb\xb",""
  "uxp!uvsumf!epwf"
  "t-\xb","uisff!gsf"
  "odi!ifot-!","gpvs!d"
  "bmmjoh!cjset-!","gjwf"
  "!hpme!sjoh<\xb","tjy!h"
  "ffft!b.mbzjoh-!","tfwfo!t"
  "xbot!b.txjnnjoh-\xb","fjhui"
  "!nbjet!b.njmljoh-!","ojof!mbe"
  "jft!ebodjoh-!","ufo!m"
  "pset!b.mfbqjoh-\xb","fm"
  "fwfo!jqjfst!jqjoh-!","ux"
  "fmwf!esvnnfst!esvnnjoh-!",""
  "Po!uif!","!ebz!pg!Disjtunbt!n"
  "z!usvf!mpwf!hbwf!up!nf!\xb","boe"
  "!");int putchar(int);int main(void
  ){while(l<(sizeof 0/sizeof*0-2)/2-1){
  I=0[_=!_?sizeof 0/sizeof*0-
  3:_<(sizeof(0)/sizeof*0-2)/2?
  sizeof 0/sizeof*0-2:==(sizeof(
  0)/sizeof*0-2)/2?++l,0:_<(sizeof(
  0)/sizeof(*0))-3?(_-1)==(sizeof(0)/
  sizeof*0-2)/2?sizeof 0/sizeof*0-1:_-1
  :_<sizeof(0)/sizeof*0-2?l+1:_<sizeof(0)
  /sizeof*0-1?l+(sizeof 0/sizeof(*0)-2)/2:(
  sizeof(0)/sizeof*0-2)/2l;while(*I){putchar(
  *I++-1);}}
  return 0;}
  
```

Figure 2 A good programmer writes clean code that is easy to understand and maintain, not the fewest lines of code!

TIP #10: GOOD PROGRAMMERS DON'T NECESSARILY WRITE FEWER LINES OF CODE

It is a common misconception that a good programmer can write fewer lines of code than an average programmer to do something. Don't get sucked into this idea! A good programmer has a well-thought-out and -structured code base. Variables are nicely named and encapsulated, with few global variables existing in the system. Functions should be short and concise. If the code looks confusing and it would be more clear to write more lines of code, then do so! Check out the online awards for writing the most confusing C code. A good programmer writes clean code that is easy to understand and maintain, not the fewest lines of code (Figure 2)!EDN


AUTHOR'S BIOGRAPHY



Jacob Benigo is a Certified Software Development Professional (CSDP) who specializes in the development and design of quality, robust embedded systems. He has written technical papers on embedded design methods and taught courses on programmable devices, boot-loaders, and software methods. Benigo holds bachelor's degrees in engineering and physics from Central Michigan University (Mount Pleasant, MI) and a master's degree in space-systems engineering from the University of Michigan (Ann Arbor, MI).

Per-quadrant linear amplifier distinguishes input polarity

by Marian Stofka

 The isolation amplifier circuit of Figure 1 is simple but accurate. With the values shown it converts 0 to 5V DC or low frequency signals with unity gain, but you can adjust the gain by changing R4.

In some applications, a linear amplifier is required which has different gains with regard to the polarity of the input signal. Figure 1 shows an inverting amplifier which is linear within the second and fourth quadrants of the $V_{OUT}(V_{IN})$ plane, but the magnitude of its gain in the fourth quadrant is higher compared to the second. The op amp IC1B acts as a differencing amplifier with a gain of:

$$-\frac{R_{i2}}{R_{i1}}, 1 + \frac{R_{i2}}{R_{i1}}$$

at its inverting and non-inverting inputs respectively. These gains are constant and independent of the input signal polarity.

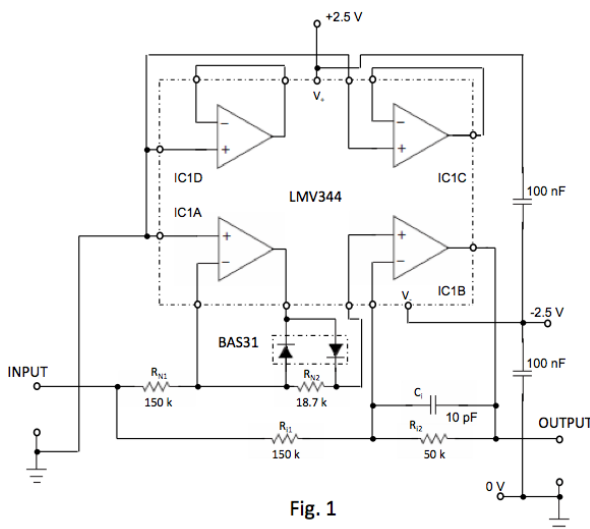


Fig. 1

Figure 1 Inverting amplifier is precisely linear within second and fourth quadrants of $V_{OUT}(V_{IN})$ plane; and has different voltage gains in these quadrants.

Polarity dependency is created in the sub-circuit built around IC1A. This sub-circuit is actually a known operational inverting half-rectifier, which outputs zero voltage for a negative input, but for a positive input, has a gain of:

$$-\frac{R_{N2}}{R_{N1}}$$

The output of the inverting half-rectifier is connected to the non-inverting input of IC1B. The output signal of IC1B for positive polarity inputs, V_{IN+} , therefore is:

$$V_{OUT} = \left(-\frac{R_{i2}}{R_{i1}} - \frac{R_{N2}}{R_{N1}} \times \left(1 + \frac{R_{i2}}{R_{i1}} \right) \right) \times V_{IN+}$$

From the required gain for positive input polarity, $A_4 = V_{OUT}/V_{IN+}$, the ratio of R_{N2}/R_{N1} can be calculated, since the ratio of

$$\frac{R_{i2}}{R_{i1}} = |A_2|$$

equals the magnitude of gain required for negative input voltages, V_{IN-} :

$$\frac{R_{N2}}{R_{N1}} = \frac{|A_4| - |A_2|}{1 + |A_2|}$$

For values of resistors given in Figure 1, the magnitudes of gain are 1/3 and 1/2 respectively.

Here the magnitudes of gain are lower than 1, but can be made higher than 1 too. The only limitation is that the magnitude of gain in the 4th quadrant is higher than its counterpart in the 2nd quadrant, as illustrated in Figure 2. If, contrarily, you need higher gain in the 2nd quadrant, simply change the polarity of both diodes in the half-wave rectifier.

Ci serves as a frequency compensation of gain. Only one half of the quad op-amp is used for the circuit, leaving two amplifiers for other uses.

Multiple PSUs share load

by Vardan Antonyan



In some projects, we need to deliver more power than a single power supply can provide, and in this situation we can use steering Schottky diodes to provide load balancing (Figure 1). In this schematic, we combine the output currents to provide some simple load sharing. Note that this is different from power redundancy, but instead the case where total output power cannot be delivered by a single power supply. This circuit is simple enough, and will work in ideal conditions where $VPS2 = VPS1$. What happens on the production floor is much more interesting, and invalidates this approach.

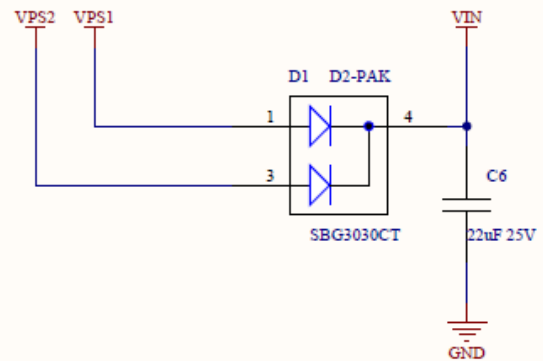


Figure 1 Two power supplies of equal voltage drive the load in current-share mode.

To evaluate the circuit, we can use the formula for Schottky diode forward voltage calculation at different currents to analyse the circuit performance at different loads and power supply deviations.

$$I = I_{SAT} \left(e^{\frac{q(V-IR_s)}{nKT}} - 1 \right)$$

The problem is that this formula is a good approximation only, and you need to use appropriate n to get similar results to diode manufacturers' V-I graph (in this case, n was selected to be 10). The analysis proved a little harder than expected since we have to consider two different power supplies, and calculate currents in an iterative manner. To solve this, we used multiple iterations using C (download available below) to calculate currents and voltages for this circuit.

The results were disappointing, since they show that in the case of $\pm 1\%$ voltage deviation, 90% of the power is supplied by a single supply. Basically, this circuit is not a good solution for power supplies with more than a few tens of millivolts difference. The problem is that not all off-the-shelf power supplies have output voltage adjustments – especially not the sealed ones. To solve this issue, a circuit was developed to ensure load sharing using off-the-shelf power supplies and components (Figure 2).

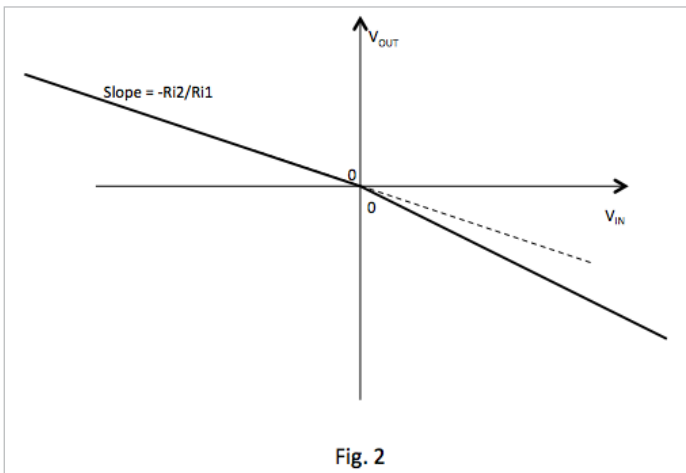


Fig. 2

Figure 2 Theoretical $V_{in}-V_{out}$ characteristic of the amplifier.

This design is intended for a compensation circuit, where parasitic pulses to be compensated have different amplitudes with regard to their polarity.

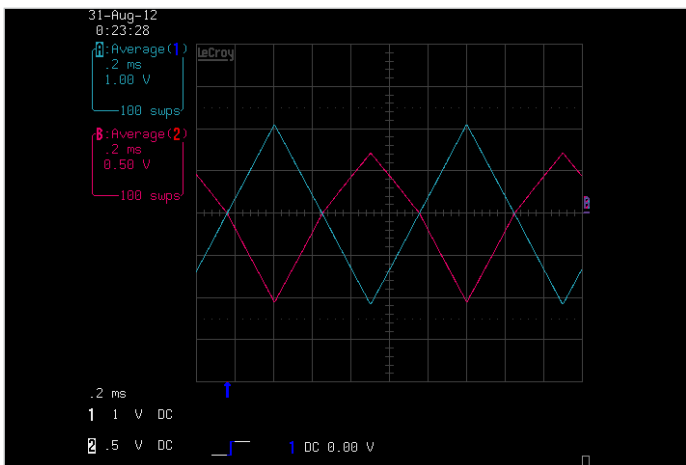


Figure 3 Output of circuit (purple trace) with a triangular input voltage waveform (blue trace) of 1 kHz.

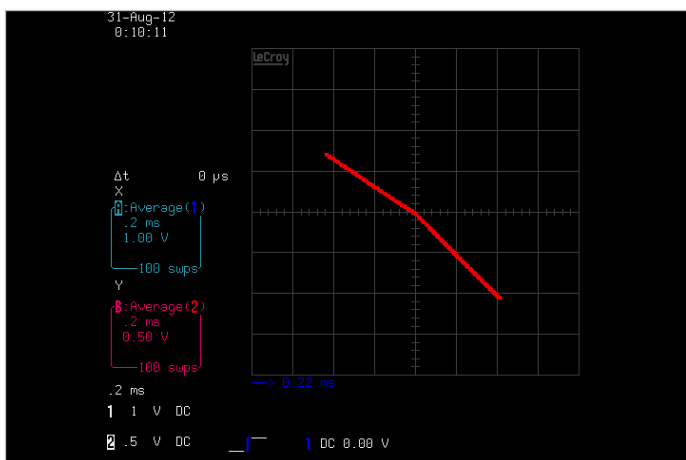


Figure 4 Input-Output ("X-Y") characteristic of the realised amplifier. Voltage gains are $-1/3$ and $-1/2$ in the 2nd and 4th quadrants, respectively.

Dr. Marian Stofka is with the Slovak University of Technology, Faculty of Electrical Engineering and Information Technology in Bratislava, Slovak Republic.

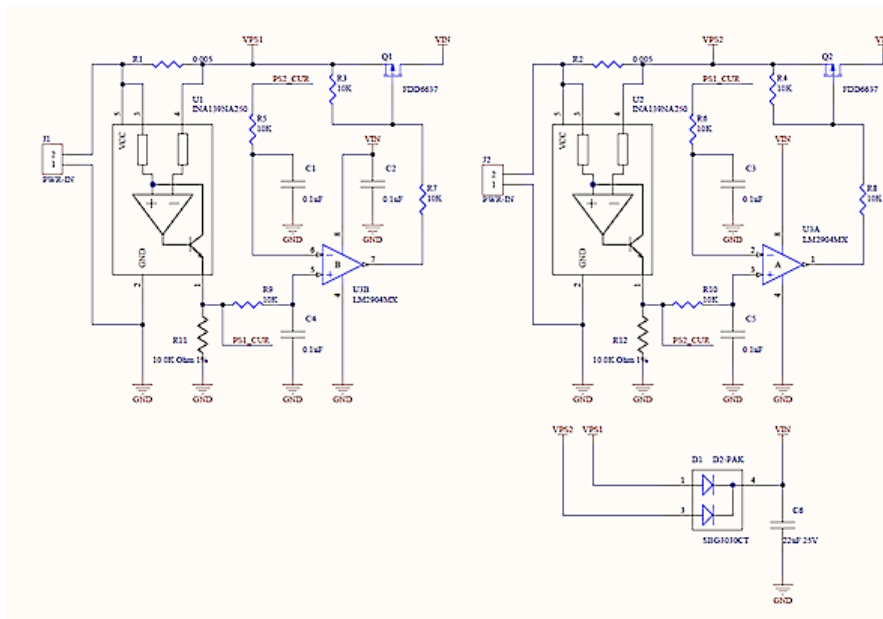


Figure 2 High-side current monitors U1 and U2 sense each supply's current, and cross-coupled control of Q1 and Q2 equalizes the current sourced by each supply.

J1 and J2 are connected to input power supplies, and the load is connected to V_{IN}. As shown, in addition to the original power steering diodes, we now also have Q1 and Q2 MOSFETs shunting the diodes to regulate load sharing. The MOSFETs are driven by U3B and U3A op-amps, each configured to compare the current of its own supply with that of the other. The circuit

does not have any stringent requirements, but R1, R11, R2, and R12 should have 1% tolerance. The op-amps are driven from simple RC low pass filters to smooth out any transient response. We use U1 and U2 to measure the current at each power supply output, and use the RC filter-amplifier-MOSFET combination to equalize the currents. This solution has been proven to work for 12V-19V input voltages (common laptop power supplies), and used to provide 10A current to the load. Load sharing efficiency is good enough to allow cascading of these circuits to combine four power supplies. See the tables 1 and 2 below for circuit performance results.

LINKS;

- Schottky Diodes (the source of the diode formula, and other Schottky information)
- C program and;
- Analysis spreadsheet

Vardan Antonyan was born in Iran, grew up in Armenia and is now living in the USA; he has followed a career path that has included electronics technician, junior Hardware engineer, Hardware engineer and then Senior Hardware engineer. During a career span of over 15 years he has been involved with all aspects of Analogue, Digital and programming in Verilog, VHDL, and C.

With Just Diodes(Figure 1)							
	Test	PS1	PS2	I load	Vload	Power	Loss Total
Vin(V)	1	20.5	20.3	1.0	20.1	20.1	3.1
	2	20.4	20.3	2.5	20.0	50.0	4.0
	3	20.4	20.3	5.0	19.9	99.3	4.7
Iin(A)	1	1.1	0.1				
	2	2.4	0.3				
	3	3.9	1.2				
Pwin(Wt)	1	22.1	1.1				
	2	48.2	5.8				
	3	79.6	24.3				
Load %	1	95.0	4.9				
	2	89.3	10.6				
	3	76.5	23.4				

Table 1

With Load Sharing(Figure 2)							
	Test	PS1	PS2	I load(A)	Vload(V)	Power(Wt)	Total Loss(Wt)
Vin(V)	1	20.5	20.3	1.0	20.2	20.2	3.2
	2	20.5	20.3	2.5	20.1	50.2	3.1
	3	20.4	20.2	5.0	20.0	100.2	7.5
Iin(A)	1	0.6	0.6				
	2	1.3	1.3				
	3	2.6	2.7				
Pwin(Wt)	1	11.6	11.8				
	2	26.2	27.1				
	3	53.3	54.3				
Load %	1	49.7	50.2				
	2	49.1	50.8				
	3	49.5	50.4				

Table 2

Novel Q-meter

Louis Vlemincq



This instrument determines the Q (quality factor) of a resonant circuit, crystal, or resonator by measuring its series resistance at the resonance frequency. The Q is linked to the series resistance by two simple equations (Rs is the series

resistance, L and C the reactive elements and Fr their resonance frequency):

$$Q = \frac{2\pi F_r L}{R_s} \quad \text{and} \quad Q = \frac{1}{2\pi F_r C R_s}$$

This Q-meter is unusual on more than one count: it is capable of displaying directly the value of the series resistance, and is based on a series-tuned oscillator. The advantages associated with this type of oscillator have been described in another de-

sign idea: Series-LC-tank VCO breaks tuning-range records
Here the series-tuned topology shines because it introduces no damping of its own at the common node between L and C, and because the tank's series resistance is accurately cancelled by a calibrated negative resistance. This negative resistance is therefore an accurate image of the resonant circuit's losses, and nothing else.

CIRCUIT DESCRIPTION

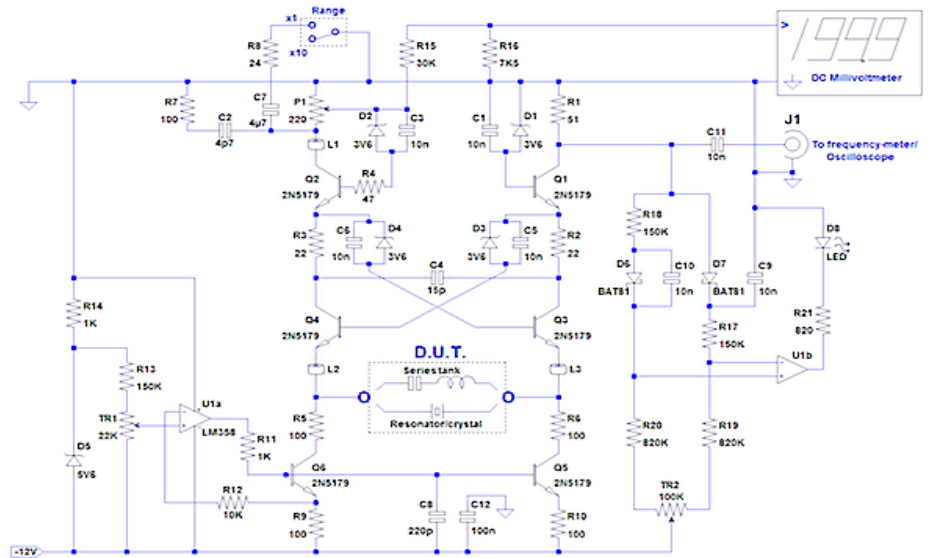
The circuit is based on the cross-quad topology(1): Q1 to Q4 form the quadruplet, and the circuit normally synthesises a zero resistance between the emitters of Q3 and Q4, by cancelling parasitic parameters.

Here, to use the circuit as an oscillator, some modifications have been made: the Zeners D1 to D4 ensure the transistors have enough C-E dynamic to "breathe" properly, and an adjustable positive feedback is introduced via pot P1 (yes, positive feedback is introduced from the collector of Q2 to its base; that's how things work in the strange and inverted world of the cross-quad).

With this modification, the resistance between the wiper of P1 and ground appears with an opposite sign between the emitters of Q3 and Q4. When the magnitude of this resistance equals that of the tank circuit, the circuit starts to oscillate. The current in the other arm of the quad is intercepted by R1, and results in a voltage appearing on the diode detector D6/D7, and the output J1. D7 is a peak detector compensated by D6. When a signal is detected, it increases the voltage on the (-) input of U1b, and pulls the output down, lighting D8.

The cross-quad is biased by two current sources, Q5 and Q6, delivering precisely 5 mA thanks to U1a. This bias current also flows through P1, and generates a voltage drop equal to the setting of the potentiometer times 5 mA.

This voltage is divided by five by R15/R16, and sent to a millivoltmeter; the value displayed in mV now reflects exactly the potentiometer's value in Ohms. Thanks to this trick, the actual value can be displayed accurately, without having to resort to approximate scales or further calculations. The resonant frequency can be measured by connecting a frequency meter to J1.



The x1/x10 switch can reduce the potentiometer's apparent value by paralleling R8, bringing the full scale value to 22Ω instead of 220Ω. Because C7 blocks the DC, the displayed value is unaffected and retains its full resolution.

The role of many components has remained unexplained so far: L1 to L3, R2 to R7, C2, C4. They all contribute to the stability of the circuit, and suppress unwanted oscillations. Without them, the circuit could oscillate at UHF frequencies; the few centimetres of the test terminals form an open transmission line having resonant frequencies of its own, and since it has a very high Q, it would invariably dominate.

The additional components constrain the frequency range: here, the maximum usable frequency is about 100MHz (to keep an acceptable accuracy). It is a trade-off between performance and usability. L1 to L3 are ferrite beads of ~80 nH (50Ω). Needless to say that careful layout techniques are a must for a stable, proper operation.

ADJUSTMENTS

In the absence of oscillation, TR2 has to be adjusted to keep the LED D8 just off, so that it lights as soon as an oscillation is present.



designideas

To adjust TR1, use a high quality tuned circuit in the 1 to 10 MHz range (polystyrene or silver mica capacitor, low loss inductor). Preset TR1 to read 0.5V between its wiper and -12V. Measure the resonant circuit on the 22 Ω (x1) range and note the value. Add a non-inductive 10 Ω precision resistor in series with the LC. Adjust P1 to the new value, and adjust TR1 to read 10 Ω plus the initially measured value. Go through the procedure again: it normally converges very quickly, and one or two passes should be sufficient. Check that the indications remain consistent in the x10 range.

PRACTICAL TIPS

With some types of components, ambiguities can sometimes appear: this is the case for low-frequency circuits and some types of resonators.

At low frequencies, the components are physically large, and the inductor has a significant parallel capacitance. The wiring and this capacitance thus form a “phantom” resonant circuit of a much higher frequency. It also has a higher Q than the “regular” circuit, because low-frequency inductors have a high ESR. All of this means that the tester will find the VHF resonance first; that is not a malfunction of the circuit, it is perfectly normal.

To force the circuit to operate at low frequencies only, the solution is to “kill” the HF response by including large ferrite beads in the circuit. The photograph

shows a practical way of implementing it: the test terminals are screw terminals directly attached to the PCB. For VHF operation, they can be used directly, but for general-purpose use, they are extended with alligator clips which are more convenient, and a large ferrite bead (1 μ H/600 Ω) is added in series with each connection. This effectively forces the circuit to operate at frequencies below 10 MHz.

The same type of problem can appear with mechanical resonators: the motional parameters are shunted by the physical capacitance, and this capacitance can resonate with the connection length. That is particularly true for ceramic resonators, having a much larger capacitance than crystals. The remedy is the same as above: add extra HF damping with beads, or an inductor shunted by a resistor.

Crystals present a problem of their own. They have a very large Q, and as a result, a large time-constant. This tester cancels the residual losses, thus increasing the apparent Q and the time-constant to near infinity! With a correct setting of P1, the build-up of oscillations can take up to a minute. This makes the adjustment near impossible — even if you turn P1 very slowly, by the time the LED lights, you will have overshoot the right value by a large amount.

In this case, the simplest solution is to connect an oscilloscope to J1, and manually act as a “human AGC” by

looking at the amplitude: the phenomena are so slow that it is easy to do. The oscillator behaves like a perfect integrator.

OTHER APPLICATIONS

Because of its inherent cancellation of parasitic parameters, this oscillator topology offers an outstanding stability, which can be used in other applications—proximity detectors for example—inductive if the coil is the sense element, or capacitive if the common node between the L and the C is the input.

It also finds the exact natural (series) resonance of a crystal very accurately, regardless of parasitic elements like shunt capacitance.

REFERENCES:

1. Precision Differential Voltage-Current Converter by Caprio; Electronics Letters, Mar. 22, 1973, vol. 9, No. 6
2. Translinear Circuits (see pg. 16 for more about the cross-quad)

Louis Vlemincq started electronics as a young teenager, first as a hobby, then as a full-time job after graduating. He has touched almost every field of electronics: audio and video design and maintenance, automotive, industrial control, lasers, telecommunications, etc. He currently works as a physical layer specialist for DSL technologies (copper) at Belgacom, the main telecom operator in Belgium.

The logo for EDN Europe features the letters 'EDN' in a large, bold, red, sans-serif font. To the right of 'EDN' is a large, light blue circle. Below 'EDN' and the circle, the word 'europe' is written in a white, lowercase, sans-serif font with a slight shadow effect. The entire logo is set against a blue background with a horizontal white stripe behind the word 'europe'.

Teardown: Samsung Galaxy Note 3 still the category leader

In 2011 Samsung defined a new category with its 5.3-in. diagonal Galaxy Note phone. The original Note was so large it was considered by many as a phone that aspired to be a tablet, hence the term "phablet" was coined.

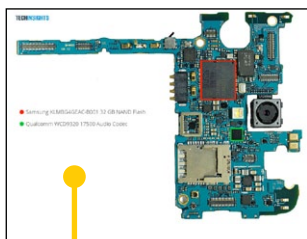
The Galaxy Note's monstrous screen was so out of place in the phone marketplace that the competition didn't even mount a comparable rebuttal for nearly 12 months. Now nearly every manufacturer offers a five-inch plus device. But they all still struggle to unseat the category leader.

With the third iteration of the Galaxy Note, Samsung has refused to add kitschy features. Rather it has focused on improving the human interaction elements in using this device as an all-in-one communications device. First off the "S-Pen" continues to be linked into more of the embedded Samsung software and features, while the new Galaxy Watch promises further improvements to the ways the user interacts with the device's proven functionality.

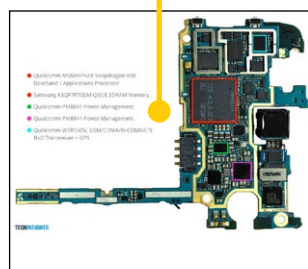
This TechInsights teardown isn't about the software updates. Rather our interest continues to lie under the hood. With that in mind, we crack open the Galaxy Note 3 to examine the horsepower needed to bring all these features to bear for the device's user.



Removing the Galaxy Note 3 board



Galaxy Note 3 board back



Galaxy Note 3 board front

DESIGN WINS AND PROCESSORS: TEARDOWN HIGHLIGHTS AND INITIAL COST ESTIMATES

TechInsights's initial bill of material costs for the Galaxy Note 3 amount to \$237.50. This is an increase of nearly \$20 over the costs of the Samsung Galaxy Note 2 HSPA device. We estimate this increase in cost is directly related to the improved and larger display module of 5.7 in. versus the previous version at 5.5 in. and the use of the Qualcomm MSM8974 baseband/applications processor. Other significant improvements are also noted in the NAND and SDRAM where the amount of memory has increased by 100% and 50% respectively.

To provide a reference of how the Galaxy Note 3 compares, we have included a comparative view against the previous generation (Galaxy Note 2 (2012)) and the recently launched Samsung Galaxy S4 LTE smart phone.

Manufacturer	Package Mark	Part Number	Description
Qualcomm	MSM8974 7AB	MSM8974AB	Snapdragon 800 Baseband / Applications Processor
Samsung	K3QF7F70DM-QGCE	K3QF7F70DM-QGCE	3GB LPDDR3 SDRAM Memory
Samsung	KLMBG4GEAC-B001	KLMBG4GEAC-B001	32 GB NAND Flash
Murata ?	0154A1 D814A7	0154A1 D814A7	WiFi/Bluetooth Front-End Module ? (Broadcom BCM433x inside ?)
Qualcomm	WTR1605L	WTR1605L	GSM/CDMA/W-CDMA/LTE Rx/Tx Transceiver + GPS
Murata	SWF / GPF10	SWF GPF10 ?	Antenna Switch w/ Duplexers & Filters
Wacom	W9010	W9010	Digitizer Controller Module? - vs. W9001 in Note II
Qualcomm	PM8941	PM8941	Power Management
Maxim	MAX77804	MAX77804	Power Management, vs. MAX77803 found in Galaxy S4 LTE
Invensense	MP65M F498E1	MPU-6500	6-Axis MEMS Gyroscope & Accelerometer
Qualcomm	PM8841	PM8841	Power Management
Broadcom	20794MA/KML08G/TD1330	BCM20794	NFC Controller
STMicro ?	32F401B / AS024VQ	STM32F401B ?	Microcontroller ?
Qualcomm	WCD9320 NGP17500	WCD9320	Audio CODEC
Qualcomm	QFE1100 D4L982	QFE1100	Power Management
Avago	ACPM-7600	ACPM-7600	Multi-mode / Multi-band Power Amp
Silicon image	8340B0	SIL8240	MHL 2.0 Transmitter w/ HDMI Input
Audience	325A/2774/321A	e5325	Voice Processor
Avago	AM3V / 9143	ACMD-6207	LTE Band VII FBAR Duplexer
Avago	A?AD / 9420	9420 ?	?? Duplexer
RF Micro Devices	RF1119	RF1119	Antenna Control Module
Micron	QCA34	M25Pxx	Serial Flash Memory
Unknown	91 / 325	91 325 ?	Receive Diversity Switch ?

Major design wins

TechInsights has noted design wins from the following integrated circuit manufacturers. The following are highlighted in the board shots we have gathered from the device.

PROCESSOR: QUALCOMM STILL THE BENCHMARK SOLUTION

Qualcomm secures the baseband/applications processor design within the Samsung Galaxy Note 3 with the Snapdragon 800, package MSM89747AB.

Manufactured in TSMC's 28 nm HPM process, the MSM8974 is the new flagship applications/baseband processor from Qualcomm. Marketed as the 'Snapdragon 800', it features four processor cores and an LPDDR3 interface. It has design wins with several high-end smart phones, including Samsung's Galaxy S4 LTE-A and now the Galaxy Note 3 N9005 LTE. With fierce direct competition from Nvidia and vertically integrated vendors like Apple, Qualcomm continues to push the limits of performance

through architectural changes and the use of advanced process nodes.

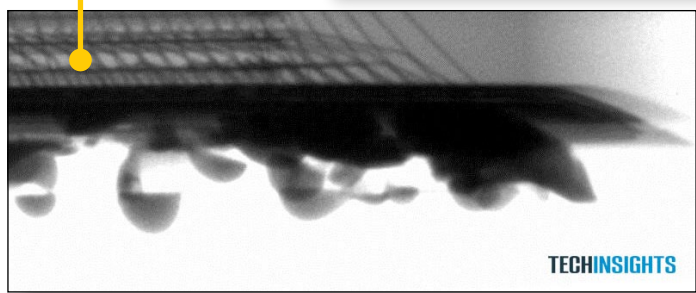
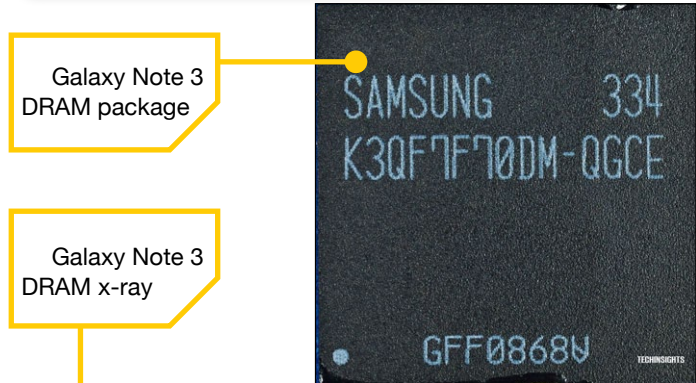
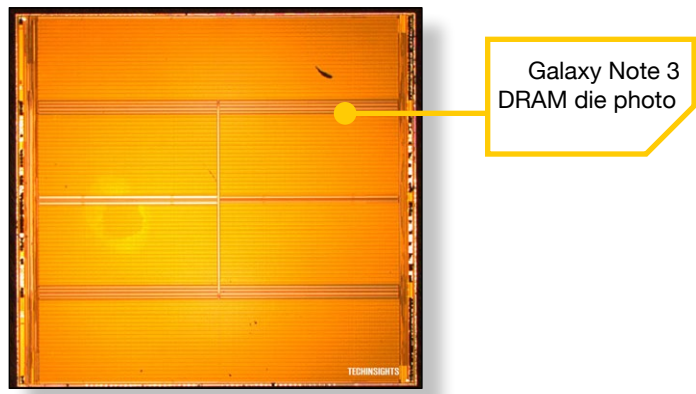
Comparing die photos and die marks, the MSM8974 looks identical to the one TechInsights previously analysed (although the previous device was marked 2012, and this one is marked 2013).

Additional information on the Qualcomm range of processors with detailed process and technical analysis can be found here:

- Logic Detailed Structural Analysis of the Qualcomm MSM8974 Snapdragon 800 SoC
- IC Design Overview of the Qualcomm MSM8974 Snapdragon 800 Processor

MEMORY: SAMSUNG PACKAGES TWIN STACKS OF LPDDR3 DRAM

From the x-ray image below, we can see Samsung's packaging solution for 3 Gbit of LPDDR3. You can see the two stacks of three dice, each wire bonded to the memory substrate. Although there is still plenty of talk about moving to TSV (through-silicon-via) solutions for mobile DRAM, we can see here that wire bonding is still a viable solution.



Die size is 6.53x6.08 mm = 39.7 mm² and the Die mark is K4E4E324ED

Addition information on the Samsung range of LPDDR3 DRAM can be found here:

CircuitVision Analysis of All of the Circuitry on the Samsung K3QF2F200C-XGCE 16 GBit LPDDR3 SDRAM

DISPLAY: BETTER IMAGES ARE "PENTILE"-TASTIC

The reason this phone is special is because of its screen. The original Galaxy Note measured 5.3in. diagonally, the Galaxy Note 2 measured 5.5in., and the latest iteration stands tall at 5.7in. of Super AMOLED beauty.

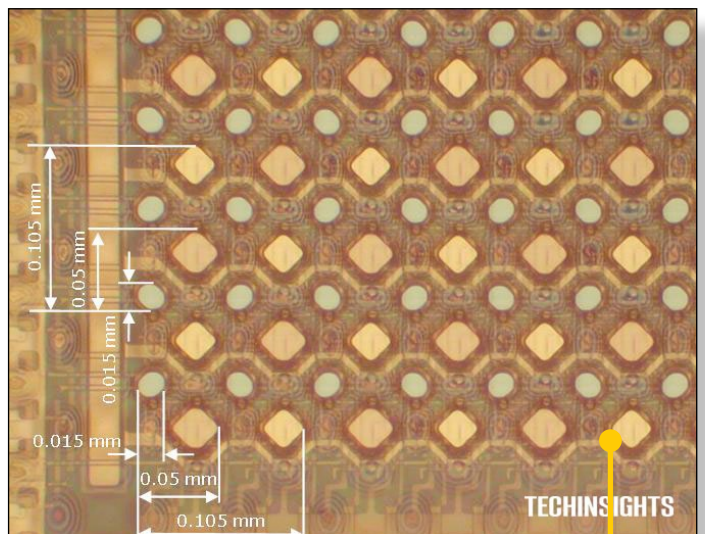
As seen in our teardown of the Galaxy S4, the Super AMOLED display is no longer an RGB matrix, but rather Samsung's PenTile. Without going into the specifics on the PenTile, the focus of Samsung with this new display technology has been to further develop the rendering of photos, videos, and screen input data while at the same time further reducing power consumption.

Addition information on the Samsung AMOLED display technology can be found at the links below.

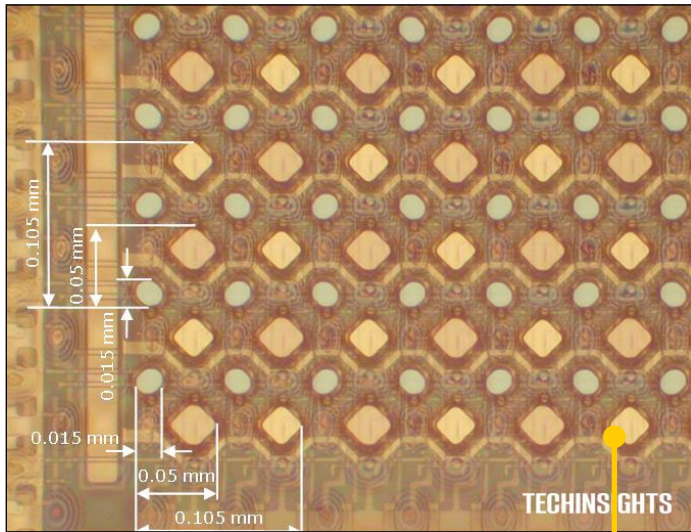
- A CircuitVision Report of the Peripheral and Pixel TFT Circuitry for the AMOLED Display in the Samsung SG-1747 Galaxy SIII Smartphone
- CircuitVision Analysis of S6E37G0X01 AMOLED Driver Circuit used in Samsung GT-I91000 Galaxy SII Smartphone

THE BILL OF MATERIALS COST: SOLID MARGINS FOR CATEGORY LEADER IN A GROWTH MARKET

Samsung's Galaxy Note 3 retails for \$699, but TechInsights Teardown costing estimates that the production of each device



Galaxy Note 3 Super AMOLED front Super AMOLED pixel dimensions, front view



Galaxy Note 3 Super AMOLED back
Super AMOLED circuit layout, back view

is less than \$240.00. Our pricing research shows that the display module and baseband processor making up the largest components of cost. This reflects a healthy margin for the industry's leading phablet device.

This number translates into the potential for significant revenues for Samsung as the Galaxy Note 2 shipped around 28



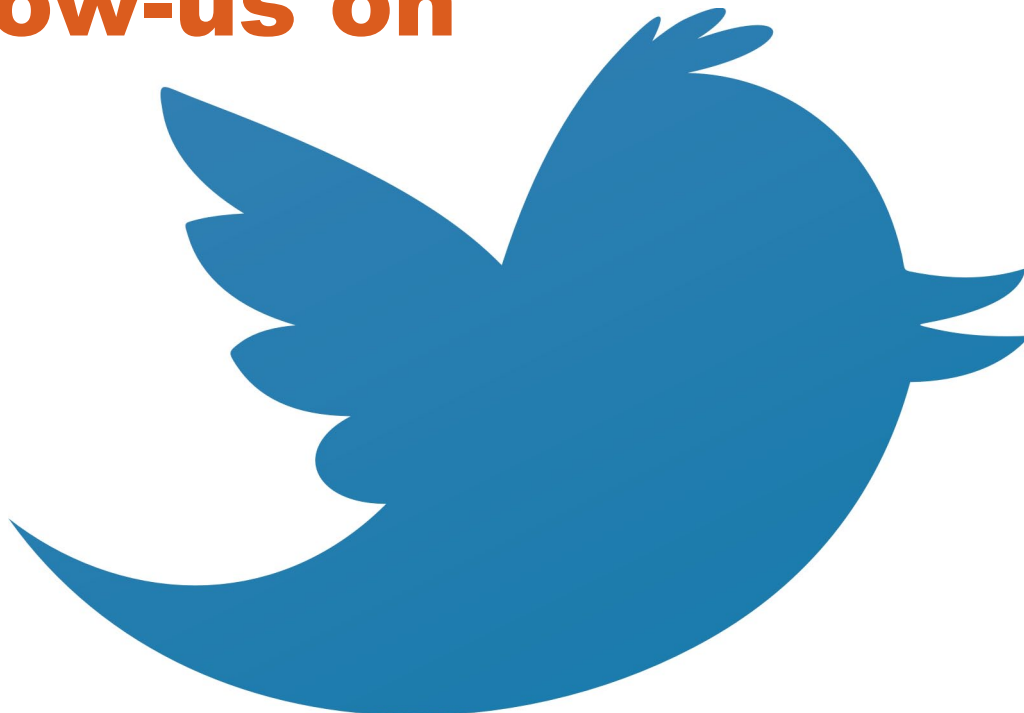
Galaxy Note 3 bill of materials comparison

million devices and combined with sales of the original Galaxy Note shipments have reached around 38 million. In fact the CEO of Samsung, JK Shin has said, "Galaxy Note 1 and Galaxy Note 2 were sold for a total of over 38 million. We believe Galaxy Note 3 will outdo its predecessors."

More to come ...

TechInsights will continue its teardown of the Samsung Galaxy Note 3...

Follow-us on



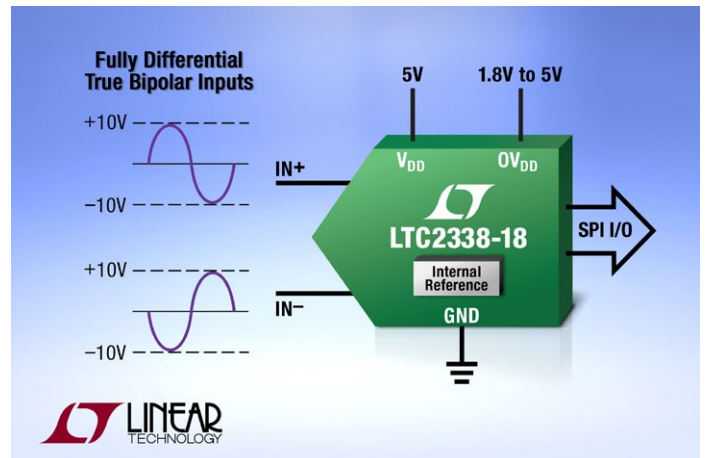
https://twitter.com/EDN_Europe

productroundup

18-bit ADC simplifies conditioning for $\pm 10V$ industrial signals

LTC2338-18 is an 18-bit, 1Msample/sec, no-latency analogue-to-digital converter (ADC) with a wide $\pm 10.24V$ fully differential, true bipolar input range for high voltage, industrial applications.

The device operates from a single 5V supply, achieves 100 dB SNR and -110 dB THD and features an internal 2.048V (20 ppm/ $^{\circ}C$ max) reference and reference buffer. An input divider network scales and level shifts the input signal, eliminating complicated circuitry required to directly interface true bipolar signals. The LTC2338-18 heads a pin- and software-compatible family of 18-bit serial SPI SAR ADCs with speeds ranging from 250 ksample/sec to 1 Msample/sec. A pin-compatible 16-bit and 18-bit family with pseudo-differential true bipolar inputs (LTC2328-18) will also be available. The proprietary internal reference buffer maintains less than 1 LSB error during sudden burst of conversions, enabling true one-shot operation after lengthy idle periods. These ADCs operate from a single 5V sup-



ply and consume 50 mW at 1 Msample/sec. A shutdown mode dissipates 300 μW when idle. Pricing begins at \$29.10 (1,000).

Linear Technology;
www.linear.com/product/LTC2338

Primary-side-control LED driver enables high PF LED lamps

Diodes Inc. has announced the AP1684, a power factor-corrected AC-DC LED driver suiting a variety of offline LED lamp types, including E26, GU10, PAR and T8. Using pulse-frequency modulation technology and operating in boundary-conduction mode, this device provides tight current regulation to an accuracy of $\pm 2\%$, while achieving a power factor of .97 and THD of less than 20%. Helping to significantly reduce circuit BOM cost,



this primary-side driver removes the need for opto-coupler, secondary-side control and loop-compensation circuitry. Driving an external bipolar junction transistor, the AP1684 requires only a small external component count and coupled with its SO8 packaging, enables lamp designers to reduce PCB footprint, increase power density and raise overall product reliability. The driver achieves high efficiency, typically 93%. The AP1684's circuit protection features include over-voltage, short-circuit and over-temperature facilities. They cost \$0.18 (50k).

Diodes;
www.diodes.com

Interface converter takes HDMI to MIPI for small screens

A chipset enables HDMI video streams to be processed and displayed on small form factor LCD displays. Toshiba Electronics' T358779XBG High Definition Multimedia Interface (HDMI) to MIPI Display Serial Interface (DSI) bridge IC is claimed to be the first device to enable HDMI video and audio output to be converted and processed as a MIPI DSI video stream for small form-factor LCD displays. The IC enables the application processors

used to drive traditional larger displays to also interface with smaller, mobile consumer and industrial products fitted with small form-factor LCD displays



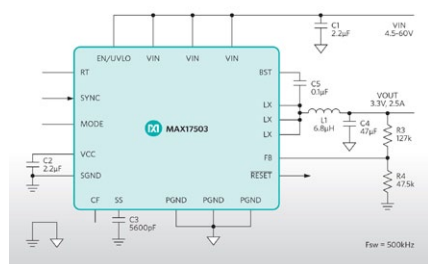
that require MIPI DSI input. By providing integrated on-chip support for video processing, video de-interlacing, video scaling and video format conversion, the T358779XBG significantly reduces memory bandwidth and video processing requirements on the host processor. Up-down scaling and colour-space conversion allows output from the application processor to be formatted and scaled to match the display panel's output resolution and colour format. Toshiba's T358779XBG supports common 3D video formats and protocols compatible with the HDMI 1.4 standard at resolutions up to 1920 x 1200 and refresh rates of 60fps.

Toshiba,
www.toshiba-components.com

60V, 2.5A voltage regulator for industrial automation designs

Maxim Integrated's high-voltage regulator reduces heat dissipation, improves reliability; reduces space by up to 50% and component count by 75%. You can achieve greater efficiency across a wide industrial voltage range with the MAX17503 synchronously-rectified DC-DC step-down converter, the company asserts. The device, which is monolithic, integrates two MOSFET switches and eliminates an external Schottky diode;

Synchronously Rectified 60VIN DC-DC Step Down Converter



the MAX17503 delivers higher power efficiency, operating 50% cooler than any other industrial high-voltage DC-DC converter. It operates from 4.5V to 60V and delivers up to 2.5A output current. The MAX17503 saves up to 50% space and

reduces component count by 75%. Internal compensation across the output voltage and 200 kHz to 2.2 MHz switching frequency range simplify the design task. The device comes in a 20-pin, 4 x 4 mm TQFN package, operates over -40°C to +125°C and costs \$1.94 (1000).

Maxim Integrated;
www.maximintegrated.com

SSDs for cost-sensitive industrial applications

Swissbit's EM-MLC (endurance managed - multi-level cell) versions of its X-500 Series Industrial SATA 2.5 in. SSD (solid-state drive) have three to ten times greater endurance while maintaining consistent data retention of up to five years, compared to standard MLC SSDs, in line with the JEDEC standard.



The X-500 EM-MLC supports a data rate (sequential read performance) of up to 240 MB/sec on SATA II and 14,800 IOPS with 4 kB random accesses. Therefore, the X-500 EM-MLC is ideally suited for cost-sensitive industrial applications that nevertheless have tough requirements, e.g. a broader temperature range between -40°C and +85°C, high shock and vibration resistance, trans-

parent diagnostic functions and advanced erase methods. As a result of specifically tested and selected MLC flash raw materials, the Swissbit EM-MLC SSD is a solution positioned between SLC (single-level cell) and standard MLC. EM-MLC X-500 SSDs are available in various densities. As with all Swissbit memory solutions, long-term availability and a fixed BOM are guaranteed for the X-500 EM-MLC SSD.

Swissbit;
www.swissbit.com

Dual full-bridge automotive motor driver IC

A4990 from Allegro MicroSystems Europe is a dual full-bridge driver IC designed to operate one bipolar stepper or two brush DC motors in automotive and harsh environment industrial applications. Each full bridge in the new device uses DMOS power devices with integrated freewheeling diodes. Peak motor current can be limited



to provide higher efficiency and reduce motor heating. The driver IC is targeted at both the automotive and the industrial markets. The A4990 enables stepper motors to be driven with full current in either direction in each phase, allowing two-phase "on" full-step operation. DC motors can be driven both clockwise and anticlockwise, and in brake mode. The A4990 is designed for typical applications requiring up to 800 mA and 28V, and has 3.3V and 5V compatible inputs. Outputs are protected from short circuits to supply and ground, and low-load current detection is included. Chip-level protection includes over-temperature shutdown and over-voltage and under-voltage lockout.

Allegro Microsystems;
www.allegromicro.com/en/Products/Motor-Driver-And-Interface-ICs/Bipolar-Stepper-Motor-Drivers/A4990.aspx

Dual-channel demod chip supports latest DVB standards

Silicon Labs' latest family of universal digital video broadcast (DVB) demodulators support worldwide DVB standards for cable, terrestrial and satellite reception. Designed to simplify the design of complex, high-performance video front-ends for integrated digital TVs (iDTVs) and set-top boxes (STBs), the Si216x/6x2 family includes

dual-channel DVB demodulators targeting multi-receiver iDTV and STB applications. The Si216x/6x2 demodulator family supports all first and second-generation DVB broadcast standards for cable (DVB-C2/C, ITU J.83 Annex A/B/C), terrestrial (DVB-T2/T) and satellite (DVB-S2/S, DSS). The Si216x/6x2 family supports the latest DVB-T2 specification (ETSI EN 302 755-V1.3.1), also known as DVB-T2-Lite. The DVB-T2-Lite specification allows simpler receiver implementations for mobile and handheld reception. The new demodulators demonstrate very short lock times in DVB-C2 mode, and they provide the industry's fastest DVB-T2 lock times, even in the presence of co-channel interference (CCI). Depending on the supported DVB standards, product pricing begins at \$6.86 (10,000) for single-channel demodulators.



Silicon Labs;
www.silabs.com/tv-demodulator

330 μ F multilayer ceramic capacitor

Taiyo Yuden has announced a 330 μ F-capacitance EIA 1210 size AMK325ABJ337MM (3.2 x 2.5 x 2.5 mm) as an addition to its super high-end product group of high-capacity multilayer ceramic capacitors (over 100 μ F). This increases capacitance by over 50% in the same size capacitor as compared to the AMK325ABJ227MM (200 μ F). The large capacitance 330 μ F super high-end product is believed to be the first of its kind. Generally, multilayer ceramic capacitors have a low ESR and superior frequency characteristics as compared to tantalum or aluminium electrolytic capacitors and are effective as smoothing capacitors for controlling the ripple current in increasingly high-frequency power circuits. Taiyou Yuden says it will continue to make further additions to its line-up of super high-end, high capacity multilayer ceramic capacitor products with a capacitance in excess of 100 μ F, and intends to progress to 1000 μ F.

Taiyo Yuden,
www.taiyo-yuden.com

FPGA family offers low cost programmable bridging

Lattice's MachXO3 FPGA family has 640 to 22K logic cells, low power, \$.01 per I/O cost, and hard IP blocks to ease implementation of emerging connectivity interfaces. The FPGA family is a small, lowest-cost-per I/O programmable platform aimed at expanding system capabilities and bridging emerging connec-



tivity interfaces using both parallel and serial I/O. By matching advanced, small-footprint packaging with on-chip resources, the MachXO3 family simplifies the implementation of emerging connectivity interfaces such as MIPI, PCIe, and GbE. The ultra-low density MachXO3 FPGA family gives customers a single programmable bridge that lets them build differentiated systems using the latest components and interface standards. The 640-to-22K logic-cell family makes use of the latest in package technology to not only deliver tiny 2.5 x 2.5 mm wafer-level chip-scale packaging, but also 540 I/O count devices, as well as devices with 3.125 Gbps SERDES capabilities. A complete MIPI based solution using hard blocks and soft IP to not only achieve high bandwidth programmable bridging for applications such as 4K x 2K video, 40MPixel image sensor interfaces, but to also enable access to the latest MIPI compliant components for advanced differentiation is paired with integrated hard PCIe, and GbE IP that enables high speed control interfaces, as well as high bandwidth data bridges.

Lattice;
www.latticesemi.com/MachXO3

Highest-isolation, carrier-grade CMOS Wi-Fi

An RF switch delivers a claimed 50 times more isolation and 10 times better linearity for 802.11ac Wi-Fi access points. Peregrine Semiconductor has announced a high-performance, carrier-grade Wi-Fi switch with the highest-available isolation – by a factor of 50. Most Wi-Fi access points now contain multiple radios in order to address the capacity demands of cellular data. Based on Peregrine's UltraCMOS technology, the PE42423 offers 41 dB of port-to-port isolation at 6 GHz. This isolation enables multi-radio access points to perform at peak levels without interference between the radios. Exceeding the stringent 802.11ac standard, Peregrine's switch also offers 65 dBm of linearity to achieve higher data rates. In addition, UltraCMOS technology delivers equally high performance at either 3.3V or 5V. The PE42423 is a Single-Pole Double Throw (SPDT) RF switch featuring low insertion loss (0.8 dB @ 2.4 GHz, 0.95 dB @ 5.8 GHz), fast switching time (500 nsec) and high ESD ratings (3.0 kV HBM on all RF pins). The switch supports +1.8V standard logic control. It provides stable RF performance over a power supply range between 2.3V and 5.5V.



Peregrine Semiconductor;
www.psemi.com

Bipolar power transistor rivals MOSFET energy efficiency

The STMicroelectronics 3STL2540 combines the cost and silicon-area efficiencies of a bipolar transistor with energy efficiency similar to MOSFETs of comparable rating, giving designers a space-saving solution for cost-conscious power-management applications and DC-DC converters.

The 3STL2540 is a -40V/-5A PNP transistor capable of full saturation with maximum voltage drop of 200 mV at 10 mA base current. It can achieve an equivalent on-resistance of only 90 m Ω , which is close to the performance of comparable super logic-level MOSFETs. ST's advanced double-metal planar base island technology enables the 3STL2540 to maintain consistently high current gain (hFE) of at least 100 over a wide output-voltage range from 0.2 to 10V and a temperature range from -30°C to 150°C, offering lowest conduction losses for this type of device. The thermally efficient PowerFLAT package is only 0.6 mm high with a 2 x 2mm footprint enabling reliable, high-performance power circuitry within minimal pc-board space. The 3STL2540 costs from \$0.30 in the PowerFLAT 2x2 package (1,000).



STMicroelectronics;
www.st.com/bipolar

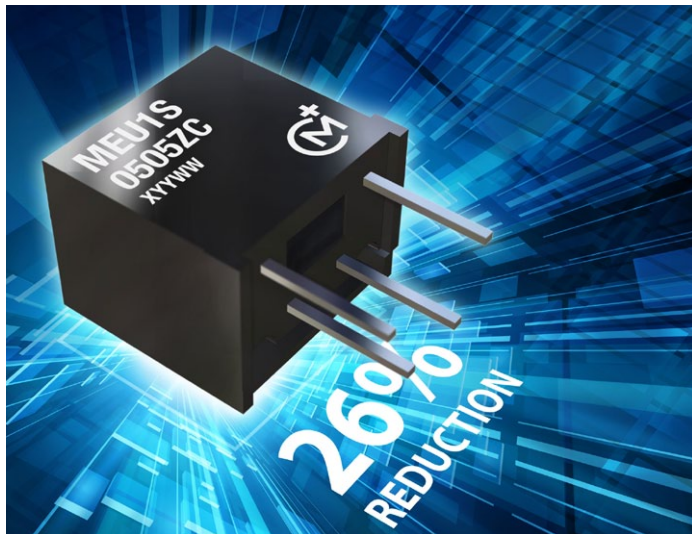
Samsung CIGT metal composite power inductors

A compact CIGT series of power inductors from Samsung Electro-Mechanics is now available from distributor TTI. These efficient devices have a monolithic structure incorporating metal composite technology with special powder and small grain size to reduce AC losses. DC losses are also lower than comparable multilayer inductors due to the use of wirewound technology using copper wire. They are magnetically shielded and extremely reliable; their small size and high efficiency saves PCB space in DC/DC power converters. Samsung CIGT composite power inductors are available in saturation currents up to 5A and inductances from 0.24 μH up to 1.0 μH . Operating temperature range is -40C to +125C. A range of sizes including a low profile type is available suit applications where PCB space is limited, such as mobile phones, tablets, LCD and AMOLED displays and storage.

TTI,
www.ttieurope.com



“Sugar-cube” 1-W DC-DC converter gets smaller still



Murata's MEU1 series of ultra miniature single isolated output 1-W DC-DC converters measures 8.30 x 6.10 x 7.55 mm, a 26% footprint reduction when compared to previously released products.

Available as through-hole mounting with staggered style pinouts, the MEU1 achieves a 25% increase in power density and can deliver its output power over the whole temperature range of -40C to +85C. Conversion efficiency has also been improved by typically 6% across the full load range compared to previous models. The MEU1 series also has load regulation that is typically 3% better than the industry norm when compared to similar miniature through-hole converters. A total of 14 models is available across the series, catering for the popular input voltages of 3.3, 5, or 12 VDC and providing outputs of 3.3, 5, 9, 12, or 15 VDC. 1-kVDC galvanic isolation aids reduction of switching noise and allows the converter to be configured to provide an isolated negative rail in systems where only positive rails exist. Certification to the international safety standard UL/IEC 60950 is pending.

Murata Power Solutions;
www.murata.eu

Portable, in-field flash programmer

Segger's Production Flash Programming line, the Flasher family, now includes the Flasher Portable, designed to fill the need of an extremely portable, production grade, Flash programmer used for in-field firmware updates. Powered by standard batteries, the Flasher Portable can be loaded with multiple firmware images. The user interface allows the user to select the firmware image to be programmed with a simple press of a button. The Flasher Portable barely ex-

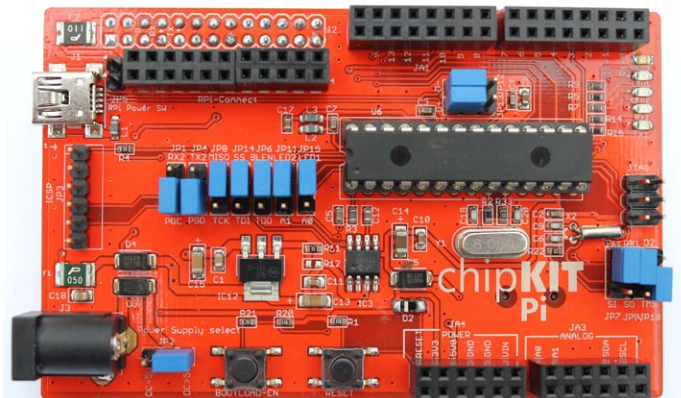


ceeds the size of a smartphone. Similar to Flasher ARM and Flasher RX, the Flasher Portable is an in-circuit programmer based on the J-Link family of debug probes using the same ultra fast flash programming algorithms. It supports targets based on ARM7/9/11, Cortex-A5/A8/A9, Cortex-M0/M1/M3/M4, Cortex-R4/R5, e200z0 (Power architecture) and Renesas RX610/RX621/RX62N/RX62T/RX630/RX631/RX63N CPUs. For a detailed list consult www.segger.com/flasher-portable.html

Segger,
www.segger.com

Arduino-compatible chipKIT Pi expansion board

Developed by distributor element14 in partnership with Microchip Technology and in collaboration with volunteers from the chipKIT and Arduino communities, the chipKIT Pi Expansion Board enables users to create, compile and program Arduino sketch-based chipKIT applications within the Raspberry Pi operating system. The board will support development of 3.3V Arduino-compatible applications for the Raspberry Pi using a 32-bit, high-performance MCU, giving access to the PIC32 MCU's performance, memory and integrated peripherals. By interfacing directly to the Raspberry Pi I/O Expansion header, users can take advantage of the large repository of available Arduino tutorials and reference materials in creating a wide array of designs. Open source tools enables users to benefit from the PIC32 MCU's high performance, memory and integrated peripherals while using the basic hobbyist prototyping equipment that is found in most home workshops.



Element14;
www.premierfarnell.com

PXIe module aids sound and vibration testing

A PXI Express dynamic signal-acquisition module, the PXIe-9529 from Adlink Technology, provides up to eight 24-bit analogue-input channels simultaneously sampling at 192 ksamples/sec with a 108-dB dynamic range for high-density, high-channel-count signal measurements. The module has a vibration-optimised lower AC cutoff frequency of 0.3 Hz,



and all input channels incorporate 4-mA bias current for IEPE signal conditioning for accelerometers and microphones. These features position the PXIe-9529 for machine-condition monitoring; noise, vibration, and harshness testing; and phased-array data acquisition. A PXI star trigger ensures synchronisation between modules with less than 1 nsec of skew. The PXIe-9529 offers input ranges of up to $\pm 10V$ or $\pm 1V$, software-selectable AC or DC coupling, and differential and pseudo-differential input configurations, with up to $\pm 42.4-V$ overvoltage protection for positive and negative inputs in both configurations. It works with Windows, LabView, MATLAB, and Visual Studio.NET and integrates seamlessly with Adlink's 3U 18-slot PXES-2780 PXI Express chassis.

Adlink Technology;
www.adlinktech.com

Noise-cancellation, zero-audible-hiss speaker driver ICs

ams has introduced the AS3435 and AS3415 ANC speaker drivers, for a new generation of noise cancellation stereo headsets with zero audible hiss; the devices are the first ANC (active noise cancellation) ICs to feature integrated bypass switches, offering headset manufacturers the freedom to create sleeker – and cheaper – industrial designs. The AS3435, for feedback systems, and AS3415, for feed-forward systems, incorporate ultra-low noise amplifiers with a 900 nV input referred noise floor: the devices are the first ANC speaker drivers to produce no audible high-frequency hiss when paired with low-noise microphones. This means that manufacturers of audiophile products can replace existing ANC solutions with the AS3435 and AS3415 to provide users with an improved listening experience, benefiting from the devices' audio characteristics including 35 mW stereo output power with THD+N of 0.1% into a 32 Ω load and a typical signal-to-noise ratio of >110 dB.

ams;
www.ams.com/ANC/AS3415 / www.ams.com/ANC/AS3435

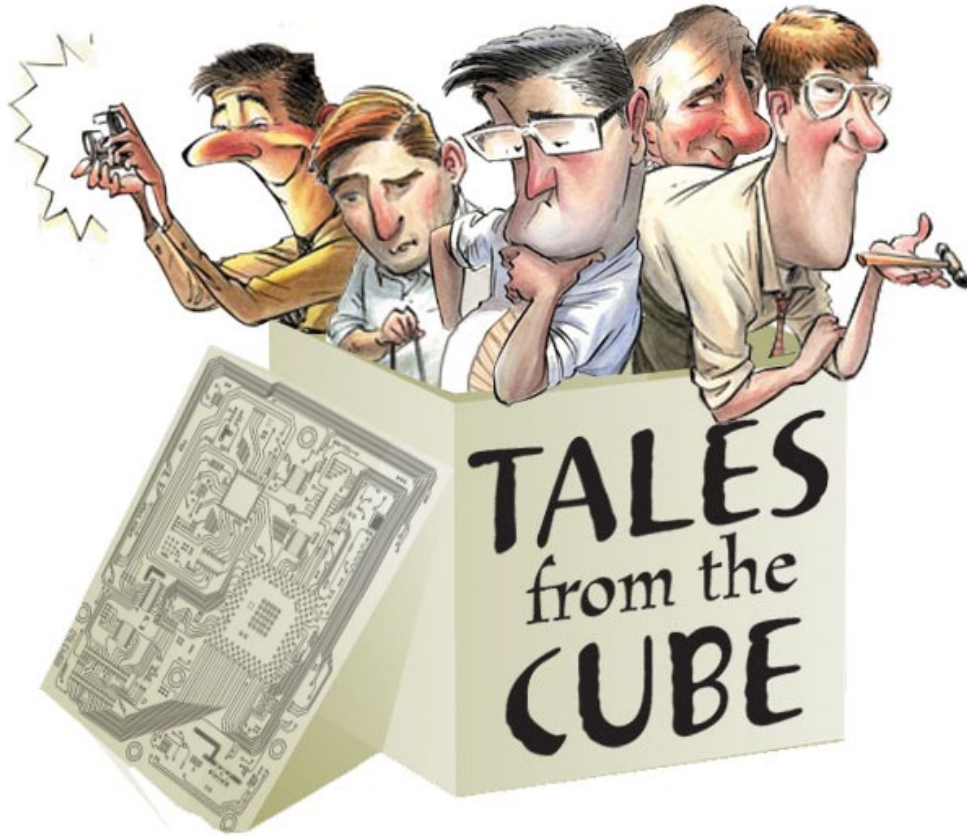
Active Noise Cancellation

- Ultra-low noise architecture eradicates hiss noise
- Unique integrated passive bypass feature

www.ams.com/ANC



A shock to the circuit



My first employment as a graduate mechanical engineer was as an assistant product engineer with Thomas A Edison Industries in West Orange, New Jersey. The job had to do with electronics packaging. Once an electronics engineer had completed a circuit design, the product engineer would do the design work to turn that circuit into a finished product. As I did this work, I became more interested in circuit design.

While working on the packaging design for a new magnetic amplifier, a real opportunity for circuit design came along, although it wasn't presented as such. One of my responsibilities involved a product that had been in production for a number of years. It had never been a problem, so I hadn't bothered to look at the design. Suddenly there was a problem and it was mine to fix. Production had assembled 600 units before doing any testing, since it had always been trouble-free, but during acceptance testing, every unit failed.

The circuit was simple: a Wheatstone bridge drove a sensitive relay, which, in turn, drove a slave relay. The input was one leg of the bridge and the output was the set of slave relay contacts. When the signal was raised to the proper level, the sensitive relay contacts were to close and energize the slave relay. The contacts of the slave relay would then light a lamp, just as in the intended application. The circuit was dead simple; small wonder there had never been a problem.

But now there was. When the slave relay closed, it did so with such force that it sent a shock through the chassis that re-opened the sensitive relay. That, of course, re-opened the slave. In time, the sensitive relay re-closed, causing the slave to re-close, and the process started all over again. The process cycle time was such that the units had become buzzers.

A phone call to the slave relay manufacturer revealed that they had "improved" the relay so as to give it a more forceful contact closure.

My engineering superiors had suggested possible fixes like adding a vibration isolator to the sensitive relay, or the slave, or both. That would require extensive development and testing of these alternatives with no assurance that any of them would work. Having the relay manufacturer make a special like the old design just for us would drive up cost. In any case, it looked like we would need a new design. The 600 units would have to be scrapped (salvaging just the relays), and our customer would not be happy with the delay in delivery.

I studied the "buzzer action" carefully. It occurred to me that since the slave relay coil was inductive, it might hold enough current long enough to stay closed until the sensitive relay re-closed if an alternate path for that current were provided. At that point, a possible fix became apparent: simply put a diode across the slave coil.

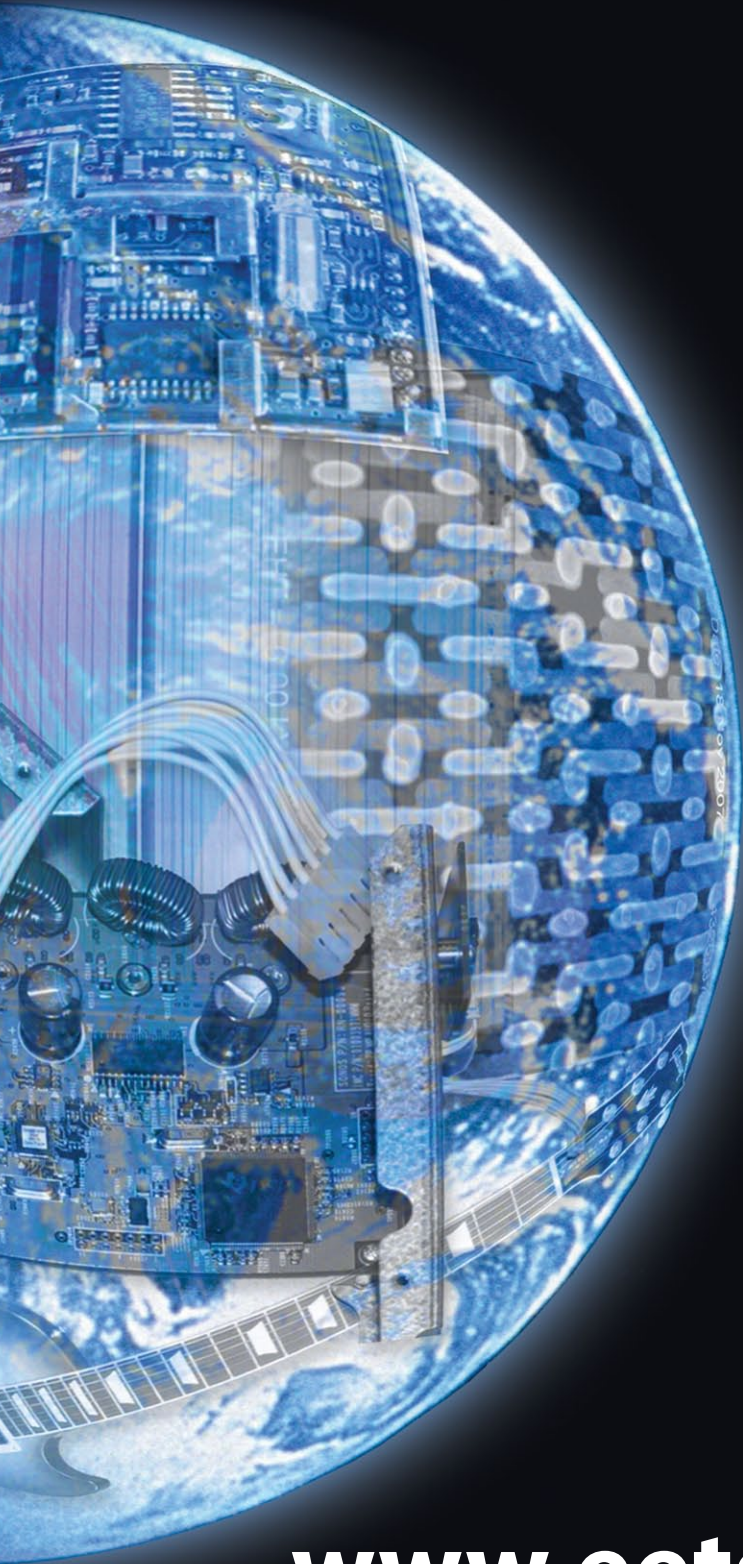
A small, axial-lead diode across the slave relay coil was all it took to get all 600 units to work properly. No redesign, scrapping, or disappointed customer, and minimal cost.

As I prepared to report my success to my bosses, I wondered what their reaction might be. After all, I had thought outside the box to save the company a lot of money, and fixed what had been presented to me as a complex mechanical problem with a simple electrical change. What would be my reward? A bonus? A commendation? Lunch? A pat on the back?

When I reported on my work, my boss said, "OK, let's get back on that mag-amp job." Apparently my reward was continued employment.

Richard Gilbert is a power electronics engineer involved with electric drives and kinetic energy recovery systems for ground vehicles.

EET Search



**- searches all
electronics sites**

**- displays only
electronics results**

**- is available on
your mobile**

www.eetsearch.com